Bull Earthquake Eng (2011) 9:199–230
DOI 10.1007/s10518-010-9238-y

ORIGINAL RESEARCH PAPER

Predicted ground motion after the L'Aquila 2009 earthquake (Italy, M_w 6.3): input spectra for seismic microzoning

B. Pace · D. Albarello · P. Boncio · M. Dolce · P. Galli · P. Messina · L. Peruzza · F. Sabetta · T. Sanò · F. Visini

Received: 24 May 2010 / Accepted: 16 December 2010 / Published online: 6 January 2011

Abstract After the April 6th 2009 L'Aquila earthquake (M_w 6.3), where 306 people died and a further 60,000 were displaced, seismic microzoning investigations have been carried out for towns affected by a macroseismic intensity equal to or greater than 7 MCS. Based upon seismotectonic data, historical seismicity and strong motion records, we defined input spectra to be used in the numerical simulations of seismic microzoning in four key municipalities, including the town of L'Aquila. We adopted two main approaches: uniform hazard response spectra are obtained by a probabilistic seismic hazard assessment introducing some time-dependency for individual faults on the study area; a deterministic design spectrum is computed from magnitude/distance pairs extracted by a stationary probabilistic analysis of historical intensities. The uniform hazard spectrum of the present Italian building code represents the third, less restrictive, response spectrum to be used for the numerical simulations in seismic microzoning. Strong motions recordings of the main shock of the L'Aquila sequence enlighten the critical role played by both the local response and distances metric for sites located above a seismogenic fault; however, these time-histories are compatible with the uncertainties of a deterministic utilization of ground motion predictive equations. As recordings at very near field are rare, they cannot be neglected while defining the seismic input. Disaggregation on the non-Possonian seismotectonic analysis and on the stationary

B. Pace (✉) · P. Boncio · F. Visini
GEOSISLAB, Università degli Studi "G.D'Annunzio", Chieti Scalo, Italy
e-mail: b.pace@unich.it

D. Albarello
Università degli Studi di Siena, Siena, Italy

M. Dolce · P. Galli · F. Sabetta · T. Sanò
Dipartimento di Protezione Civile, Rome, Italy

P. Messina
C.N.R., Istituto di Geologia Ambientale e Geoingegneria, Rome, Italy

L. Peruzza
OGS, Istituto Nazionale di Oceanografia e Geofisica Sperimentale, Sgonico, TS, Italy

site-intensity estimates reach very similar results in magnitude-distance pairs identification; we interpret this convergence as a validation of the geology-based model by historical observations.

Keywords Time-dependent probabilistic seismic hazard assessment · Site-Intensity approach · Ground Motion · Response Spectra · L'Aquila earthquake

1 Introduction

Observations of post-earthquake damage patterns often reveal substantial variability at short distances from the epicentre, as well as collapse and severe damage at great epicentral distances. Examples of these phenomena, such as the consequences of the M_w 6.3 Abruzzo earthquake occurred on April 6, 2009, were frequent in the municipality of L'Aquila (e.g. the Onna village), or even in a few relatively distant municipalities, such as S. Pio delle Camere (Castelnuovo). Construction quality is likely to play a major role in the variable levels of damage, but causes quite often have to be investigated in terms of the different local seismic amplification effects arising due to the lithostratigraphic and morphological characteristics, as studied by seismic microzoning (SM).

Depending on the different settings and purposes, SM studies can be carried out at different levels of analysis with increasing complexity, according to the following three levels (Gruppo di lavoro 2008):

- Level 1 is a preparatory level consisting of a collection of pre-existing geological, geophysical and geotechnical data analysed in order to qualitatively classify the territory into homogenous seismic microzones;
- Level 2 incorporates the quantitative elements associated with the homogenous zones and generates an SM including quantitative evaluation of expected ground motion amplification factors by using standard Vs profiles parameterized on the basis of field data collected for that purpose;
- Level 3 generates an SM map with detailed analyses (Local Seismic Response evaluations) in particular areas.

With application to the reconstruction in Abruzzo, a level 2–3 SM based on the above criteria was carried out for those towns that were affected by a macroseismic intensity equal to or greater than 7 MCS. Field activities involved about 150 researchers and experts from 8 Italian Universities (L'Aquila, Chieti-Pescara, Genova, Torino, Firenze, Basilicata, Roma1, Siena), from 7 research centres (CNR, INGV, AGI, ReLuis, ISPRA, ENEA, OGS), and from 4 regional institutions (Lazio, Emilia-Romagna, and Toscana Regions; Province of Trento). The Italian Department of Civil Protection coordinated the team.

Activities were organized under 10 thematic tasks. Among these, the results of Task 6, *Definition of Design Earthquakes for Numerical Simulations*, are the subject of this paper and were developed by the present authors. Based on seismotectonic data, historical seismicity and strong motion records, elastic response spectra were assimilated as input for the numerical simulations of the SM.

The analyses carried out for the seismic input characterization followed two different approaches:

(a) A probabilistic approach based on the combination of stationary and time-dependent seismogenic sources of the Abruzzo region, for the definition of Uniform Hazard Spectra (UHS).

(b) A deterministic approach based on the selection of a design earthquake derived from the disaggregation of the hazard, from magnitude/distance pairs extracted by probabilistic analysis of historical intensities, and from strong motion recordings acquired during the Abruzzo seismic sequence.

2 Seismotectonic context, historical seismicity and geology-based seismogenic sources

The Apennine area surrounding the L'Aquila town is a mountain region formed by ridges of prevailing carbonate rocks and intramountain tectonic depressions filled by continental deposits. The main structure of this part of the Apennines was shaped between the Late Miocene (Messinian) and the Early-Middle Pliocene by SW–NE directed compressional tectonic forces, which initiated NE-verging fold-and-thrust structures. Since Late Pliocene—Early Pleistocene times, the compressional structures have been displaced by normal faults driven by SW–NE oriented tensional forces, creating the intramountain tectonic depressions (e.g, Lavecchia et al. 1994). The extensional tectonics is presently active along the entire axial zone of the Apennines, as testified by field geology and paleoseismology (Bosi 1975; Galadini and Galli 2000; Bosi et al. 2003; Galli et al. 2008; Messina et al. 2009a), geodetic data (D'Agostino et al. 2008), instrumental seismology (Pondrelli et al. 2006) and seismotectonic studies (Pace et al. 2002; Boncio et al. 2004a). The active normal faults strike on average NW–SE, with local variations to ∼W–E or WNW–ESE, and dip to the SW or to the SSW (Fig. 1). Most of the historical earthquakes of the Apennine area can be linked to normal faulting, and the L'Aquila 2009 seismic sequence is the most recent expression of such an active tectonic process.

Geological, seismological and geodetic data indicate that the April 2009 seismic sequence reactivated two major faults of the central Apennines active normal fault systems (for geological data see Boncio et al. 2010; EMERGEO Working Group 2009; Falcucci et al. 2009a; Galli et al. 2009 Gali, 2010, ISPRA at www.apat.gov.it, Messina et al. 2009a; for seismological data see Chiarabba et al. 2009; Cirella et al. 2009; Pondrelli et al. 2009; for geodetic data see Anzidei et al. 2009; Atzori et al. 2009 and Walters et al. 2009). The April 6 main shock (M_w 6.3), and probably the April 7 strong aftershock (M_w 5.6), reactivated the SW-dipping Paganica normal fault, for a total sub-surface length of about 20 km in the NW-SE direction (fault 4 in Fig. 1). The April 9 strong aftershock (M_w 5.4) occurred about 18 km north of the main shock and reactivated the southern portion of the SW-dipping Mt. Gorzano normal fault (fault 1 in Fig. 1). The hypocentral depths were mostly within the upper 10 km of the crust, with a nucleation depth of ∼9.5 km for the April 6 main shock, but the entire range of seismogenic depths associated with the seismic sequence seem to be around 14–15 km (Chiarabba et al. 2009; Cirella et al. 2009). The main seismogenic sources dip to the SW at an average angle of 50–55° (Chiarabba et al. 2009; Pondrelli et al. 2009).

2.1 Historical seismicity

The investigated area has been struck frequently by moderate earthquakes, and by some of the strongest events ever to have occurred in central Italy.

Since its foundation in the late 13th century, L'Aquila has been hit by earthquakes several times: the Italian database of macroseismic intensities DBMI04 (Stucchi et al. 2007) reports 10 events before 2009, with site intensities Is ≥VII MCS, while heavy disruption (Is = IX MCS) occurred following events on September 9, 1349, November 27, 1461, and

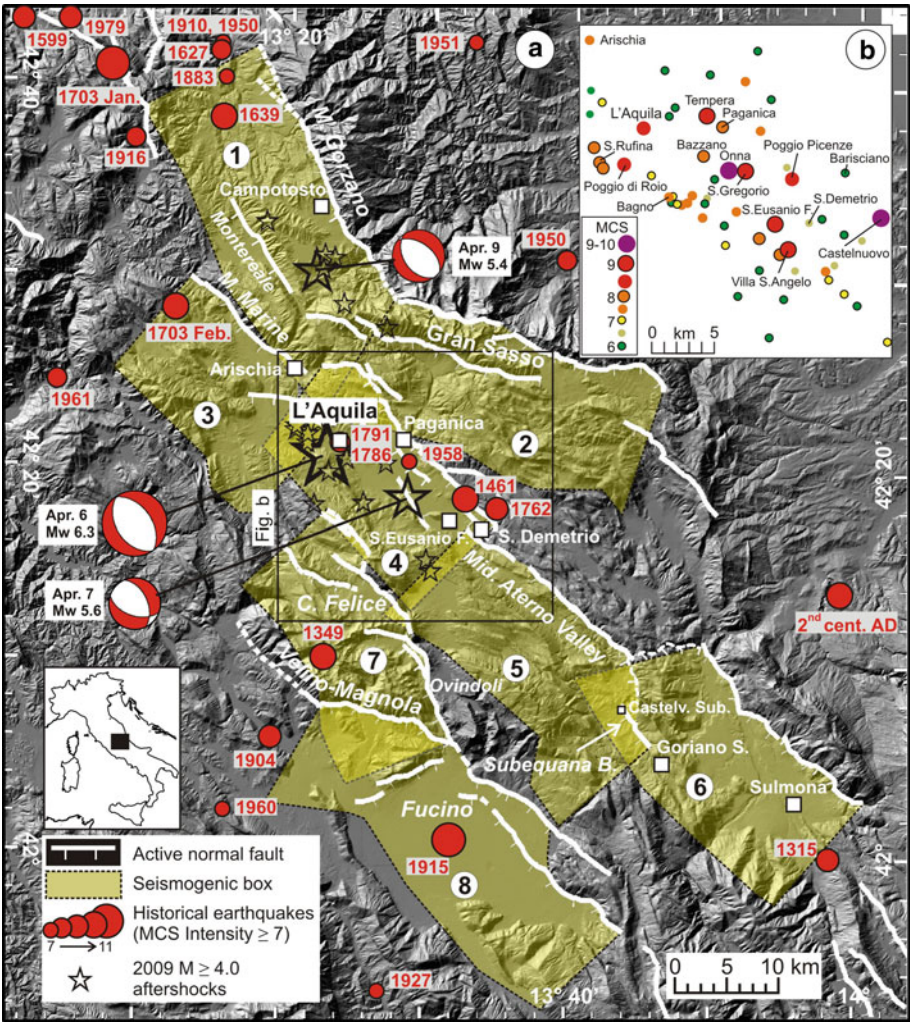

Fig. 1 Map of active faults (late Quaternary activity; i.e, Late Pleistocene—Holocene) and geology-based seismogenic sources capable of generating $M > 6.0$ earthquakes used for seismic hazard analysis. Dashed faults are segments (or the continuation of a late Quaternary fault, see Table 1 for fault parameters) constrained by structural geology but without clear evidence of late Quaternary activity. Historical earthquakes (*red full dots*) since 217 B.C.) are obtained from Working Group CPTI (2004). Main shock and aftershocks (*black open stars*) of the 2009 L'Aquila seismic sequence are from Chiarabba et al. (2009). The *inset* (Fig. 1b) represents macroseismic intensities of 2009 L'Aquila earthquake (MCS scale, from Galli and Naso 2009)

February 2, 1703. A site intensity as high as Is = VIII MCS was assigned to L'Aquila municipality during the last April 6, 2009 earthquake (Galli et al. 2009). Macroseismic earthquake catalogues (e.g, Working Group CPTI 2004—hereinafter referred as CPTI04—and reference therein), and recent studies (e.g. Rossi et al. 2005; Tertulliani et al. 2009; Galli et al. 2010) summarize the main characteristics of the local seismicity. According to Galli et al. (2010), the most important seismogenic contribution is derived from the Aterno River basin (L'Aquila—Sant'Eusanio F. area in Fig. 1), where about 40 historical earthquakes with

epicentral intensities Io≥V MCS (maximum Io = X MCS, $M_w \sim 6.4$ on 1461) have occurred. Others events originated north of Campotosto and in the Arischia area (respectively, 15 and 16 earthquakes with Io≥V MCS), where the strongest one occurred on February 2, 1703 (Io = X MCS, M_w 6.7).

In brief, after a strong but local earthquake that occurred in 1315 (M_w 6.0 in CPTI04), the first event that rocked L'Aquila, its neighbouring villages and castles, was an event in 1349 (M_w 6.5 in CPTI04). Actually, this earthquake is considered a cascade event, with separate epicentral areas involving dozens of localities spread all along the entire central-southern Apennines. While it is accepted that the strongest main shock (M_w 6.7) was generated by the Aquae Iuliae Fault (about 50 km southward of Fucino basin; Galli and Naso 2009), the subcontemporary main shock hitting the Abruzzo area (causing damage from the Salto Valley area to Sulmona, and 800 casualties in the area referred to as L'Aquila as reported by the local contemporary chronicler, Buccio di Ranallo, fourteenth century) has not yet been assigned to a known seismogenic structure. A possible association with the Campo Felice—Ovindoli seismogenic structure was proposed by Pace et al. (2006) (see Table 1).

About one century later, L'Aquila was hit again by a M_w 6.4 earthquake (CPTI04), on November the 27th, 1461. Many private and public buildings and most of the churches were razed to the ground, but thanks to some foreshocks that alerted the inhabitants, deaths were only ∼70 in L'Aquila, and less than 150 in the whole mesoseismal area (as described by the contemporary chronicles of d'Angeluccio, fifteenth century, and de Tummolillis, fifteenth century). This event rocked the same villages hit by the 2009 earthquake, and particularly Castelnuovo, Onna, Poggio Picenze and Sant'Eusanio Forconese (all with intensities IX–X MCS; see their location in Fig. 1b), as well as the more distant locality of Castelvecchio Subèquo (Is ∼ VIII–IX MCS; Galli et al. 2009); similarly to the 2009 event, there was quite a long seismic sequence lasting from November 1461 to March 1462, with several large shocks causing further damages.

More local earthquakes were felt also during the sixteenth and seventeenth centuries along the Aterno Valley, but none of them caused heavy damage. However, on February 2, 1703, a devastating earthquake (M_w 6.7) razed L'Aquila to the ground (IX MCS) along with all the villages along the Upper Aterno Valley. This earthquake happened two weeks after another main shock (January 14, M_w 6.7), which was located just a few tens of kilometers to the northwest, in the Norcia area (upper-left corner of Fig. 1); together, they represent the strongest seismic sequence that has ever occurred in this sector of the Apennines, with about 9,000 casualties. Also in this case, most of the villages struck by the 2009 event suffered comparable effects (VIII–IX MCS in Poggio Picenze, San Gregorio, Sant'Eusanio Forconese, Paganica, Bazzano, Onna, Santa Rufina, Tempera), and Castelnuovo reached X MCS. Historical accounts described the opening of long chasms along the foothill bounding the Aterno River valley; they have been investigated by means of paleoseismological analyses (Moro et al. 2002; Galli et al. 2010), thus implying the association of the February 2 shock with the Upper Aterno Fault System (seismogenic box 3 in Fig. 1).

On October 6, 1762 another earthquake hit the region but again at only a few localities (Castelnuovo, IX–X MCS; Poggio Picenze, IX MCS; Barisciano, VIII–IX MCS) already damaged by the previous events. Two other moderate shocks caused damage to L'Aquila in 1786 and in 1791 (Is–VII MCS).

During the twentieth century, an event occurred on June 24, 1958 ($M_w \sim 5$; Rossi et al. 2005), with Is = VII MCS effects felt in several villages (i.e, Bazzano, Onna, San Demetrio ne' Vestini); the mesoseismic area mimics the one that generated by the 2009 event, but scaled by several MCS degrees.

Table 1 Parameters of the geology-based seismogenic sources modelled for seismic hazard

Seismogenic source	*L* (km)	*D* (km)	*W* (km)	*A* km^2	Slip rate (mm/a) [time in kyr] (ref.)	No. paleo-eqs [time in kyr] (ref.)	Historical eqs [Mw]	M1 (RLD)	M2 (RA)	M3 (M_0)	Model slip rate (mm/a) (1s)	Model *M*	Model Tm
(1) Mt. Gorzano	28.4[a]	15.0	19.6	556	0.7–1.1 [20–30] (5) 0.5 [8.2] (5, 8) 0.7 [800] (11)	2 [8.2] (8)	1639 [6.3] Northern portion	6.6	6.7	6.7	0.7 (0.35)	6.7	1927
(2) Gran Sasso	28.7	15.0	19.6	562	0.6–1.0 [13–18] (1) 0.68 [31.5] (6)	4 [18] (1, 9) Western part	/	6.6	6.7	6.7	0.7 (0.35)	6.7	1110
(3) Mt. Marine–Mt. Pettino	21.5	14.0	18.3	393	0.3–0.4 [23–32] (5) Mt. Marine 0.5–0.9 [23–32] (5) Mt. Pettino	5 [15] (7) Mt. Marine	Feb. 1703 [6.7]	6.4	6.6	6.6	0.5 (0.1)	6.6	1213
(4) Paganica	20.0	14.0	18.3	366	0.24 [24.8] (14) 0.4 [450] (13)	Analyses in progress	1461 [6.5]	6.3	6.5	6.5	0.7 (0.1)	6.3	531
(5) Middle Aterno Valley–Subequana Basin	29.0	14.0	18.3	530	0.3–0.4 [150–250] (5) north. part 0.3 [900–1000] (this paper) central part	>1 [2.6] (15) Subequana Basin	/	6.6	6.7	6.7	0.3 (0.15)	6.7	2660
(6) Sulmona	23.5	15.0	19.6	460	0.5–0.7 [900–1000] (5) 0.4–0.8 [36–60] (12)	No data	II cent. AD (?)	6.5	6.6	6.6	0.7 (0.1)	6.6	996

Table 1 continued

Seismogenic source	L (km)	D (km)	W (km)	A km^2	Slip rate (mm/a) [time in kyr] (ref.)	No. paleo-eqs [time in kyr] (ref.)	Historical eqs [Mw]	M1 (RLD)	M2 (RA)	M3 (M_0)	Model slip rate (mm/a) (1s)	Model M	Model Tm
(7) C. Felice–Ovindoli	26.5	13.0	17.0	449	0.8–1.4 [250] (5) C. Felice 1.1 [18] (5) C. Felice 0.8–1.2 [7] (2)	3 [7] (2)	1349 [6.5] (?)	6.5	6.6	6.7	1.0 (0.1)	6.7	788
(8) Fucino	38.0	13.0	17.0	645	0.4 [400] (5) Marsicana f. 0.5–1.0 [10–18] (4) Parasano 0.5–1.4 [10–18] (4) Serrone 0.7–0.8 [900–1000] (5) Magnola 0.4–1.0 [10–18] (4) Magnola	9 [19.8] (3)	1915 [7.0] 508 AD	6.8	6.8	6.9	1.0 (0.1)	7.0	1256

L fault length; D thickness of the seismogenic layer; W down-dip length (calculated for an average dip of 50°); A fault area (LxW). Slip rate are the minimum values of the vertical component (i.e., throw rates). The number of paleoearthquakes recognized on the faults in the time span reported in square brackets (in kyr) are referenced (ref.) like that: (1) Giraudi and Frezzotti (1995); (2) Pantosti et al. (1996); (3) Galadini and Galli (1999); (4) Piccardi et al. (1999); (5) Galadini and Galli (2000); (6) Galli et al. (2002); (7) Moro et al. (2002); (8) Galadini and Galli (2003); (9) Galadini et al. (2003); (10) Salvi et al. (2003); (11) Boncio et al. (2004b); (12) Gori et al. (2009); (13) Messina et al. (2009b); (14) Boncio et al. (2010); (15) Falcucci et al. (2009b). Historical associated earthquakes with date and M_w are taken from Working Group CPTI (2004); question marks for historical earthquakes indicate doubtful association. M1 and M2 are maximum magnitudes from Wells and Coppersmith (1994) empirical relationships from subsurface rupture length (RLD) and rupture area (RA), respectively; M3 is the maximum magnitude from the expected scalar seismic moment (M_0), under the assumption of constant strain drop (3×10^{-5}; Selvaggi 1998). Model slip rate (the 1 σ uncertainty is indicated in brackets), Model M (magnitude) and Model T_m (average recurrence time of the maximum expected earthquake) are the values used for seismic hazard analysis

[a] The length of the M. Gorzano normal fault includes the 20 km-long segment showing clear evidence of late Quaternary faulting (Galadini and Galli 2000) plus the continuation to the NW of the same structure, without constraints on late Quaternary faulting, based on structural geology analyses (along-strike variation of Quaternary displacements; Boncio et al. 2004a)

Outside broad Aterno Valley area (as described above), a strong contribution to the seismic hazard of the investigated zones is derived from the earthquakes generated by the Fucino Fault System, such as the January 13, 1915 M_w 7 event. The effects of this earthquake were dramatic (Io XI MCS), since it devastated most of the villages built around the ancient Fucino Lake, causing more than 33,000 deaths. In L'Aquila and surrounding villages along the Aterno River, the earthquake caused damage corresponding to degree VII–VIII MCS, and up to VIII–IX (e.g. Sant'Eusanio Forconese, Bagno Piccolo).

Finally, another strong event outside the Aterno Valley occurred in 1639 (M_w 6.3). It struck Amatrice and its surroundings village, and has been tentatively linked with the partial rupture of the Mt. Gorzano Fault (Castelli et al. 2002; Boncio et al. 2004b).

2.2 Geology-based seismogenic sources

In order to define the earthquake potential in the study area, we considered the most important active faults, capable of generating earthquakes larger than M 6.0 (Fig. 1). The seismogenic sources employed here are derived from the integration of two previously published datasets (Galadini and Galli 2000; Boncio et al. 2004a), supplemented by data gathered by some of the present authors since 2004. The Database of Individual Seismogenic Sources DISS by INGV (http://diss.rm.ingv.it/diss/) has been not considered in this work because it is incomplete at least in this region, as confirmed by the absence of the L'Aquila 2009 earthquake seismogenic source. The model published by Boncio et al. (2004a) was used for seismic hazard analyses in central Italy by Pace et al. (2006); starting from their results, we focused our analysis only on individual sources lying within a distance of about 40–50 km from the April 6, 2009 seismogenic fault. Nearly all the major earthquakes that have occurred in the L'Aquila surroundings can be assigned to this group of faults; therefore most of the seismic potential that the national seismic hazard map (Working Group MPS 2004) can focus on is located in an elongated stripe of high hazard that can now be assigned to smallest individual patches. As we are interested in localities which are located near these faults (towns affected by a macroseismic intensity equal to or greater than 7 MCS), the contribution of more distant individual faults can be considered negligible.

The faults were parameterized in terms of length, attitude, kinematics and slip rate thanks to surface geological data (mainly from Galadini and Galli 2000). Their 3D geometry, used in shaping the seismogenic sources (seismogenic boxes, SB; Fig. 1), was defined using the approach and data of Boncio et al. (2004a); the depth distribution of seismicity, the thermomechanical constraints imposed on the bottom of the seismogenic layer, and the definition of a first-order segmentation pattern were implemented by local seismicity data of the Abruzzo region, pre- and post-2009 earthquakes (Boncio et al. 2009, and seismotectonic data from the L'Aquila sequence). This integration of previous and new data allowed us to define an updated model of seismogenic sources that slightly differs from the one described by Pace et al. (2006). In particular, the geometries of the Paganica and Middle Aterno Valley sources (no. 4 and 5 in Fig. 1; nos. 12 and 13 in Pace et al. 2006) were modified according to the seismotectonics of the L'Aquila 2009 earthquake. The Fucino SB (no. 8 in Fig. 1; no. 22 in Pace et al. 2006) now incorporates the eastern portion of the SB no. 20 (Velino-Magnola) of Pace et al. 2006, in order to obtain a better match between the calculated seismogenic potential and the magnitude of the 1915 earthquake ($M \sim 7.0$; Galadini and Galli 2000 and references therein). The western portions of the SB no. 20 and the SB no. 10 (Montereale) described by Pace et al. (2006) were not considered here due to the continually scarce, or controversial, geological constraints regarding their primary seismogenic role.

The geometric and kinematic parameters of each geology-based seismogenic source are summarized in Table 1. All the faults are constrained by detailed geological and morphotectonic studies aimed at ascertaining their repeated activity during the late Quaternary, mostly during the last ~20 ky (see Boncio et al. 2004a and Galli et al. 2008 for a review). The faults are also constrained by at least one paleoseismological trench aimed at detecting pre-historical earthquakes and the associated coseismic offsets, recurrence times and average slip rate (see Galli et al. 2008 for a review). The Sulmona fault (no. 6) is the only fault without paleoseismological data, but its present activity is documented by field evidence of repeated surface ruptures affecting post-last glacial maximum deposits (Gori et al. 2010).

Within the fault system reported in Fig. 1, we defined a first-order segmentation pattern in order to estimate the maximum expected magnitude. Consequently, we identified a set of master faults, comprising structures considered to be continuous within the seismogenic depth and that can be reactivated in their entirety during the same earthquake. The master faults of the central Apennines encompass examples of (a) large isolated fault segments (e.g. Mt. Gorzano, Sulmona) and (b) systems of closely-spaced segments, overlapping or linked by connecting structures, that are considered part of a single large structure continuous at depth (Gran Sasso, Mt. Marine—Mt. Pettino, Middle Aterno Valley—Subequana Basin, Campo Felice—Ovindoli and Fucino systems). The April 6, 2009 earthquake is an example of closely-spaced, right-stepping segments joining at depth into a continuous fault that ruptured during a single large earthquake. Paleoseismological data help in defining the master fault, when the same event is recognized on different segments of the system (e.g. Fucino: Michetti et al. 1996; Galadini and Galli 1999; or Campo Felice—Ovindoli: Pantosti et al. 1996; Salvi et al. 2003). The most uncertain structure, in terms of along-strike continuity at depth, is the Middle Aterno Valley—Subequana Basin system, which includes two main faults (Fig. 1): the Middle Aterno fault can be reasonably considered a continuous SE-striking major fault about 20 km long (Galadini and Galli 2000); the Subequana Basin fault is a SE-striking fault about 5 km long, in right-stepping relationship with the Middle Aterno fault. Although the surface geology does not provide conclusive evidence for their linkage during the late Quaternary, they are considered here as linked by a connecting normal fault striking ~N-S, dipping to the W and offsetting the pre-Quaternary bedrock (APAT 2005; Vezzani and Ghisetti 1998); the total length of this hypothesized master fault is therefore 29 km. In general the master faults lengths analyzed in this paper range from 20 to 38 km (Fig. 1, Table 1).

Concerning the fault slip rates, the values reported in Table 1 are minimum values of the vertical component of slip rate (i.e, the throw rates). The throw rates range from $\geq$0.3 to 1.4 mm/a (see Table 1 for chronological intervals and references). Given the uncertainties affecting these measurements, mostly due to timing uncertainties, the reported values are considered here approximately equal to the slip rate along the fault ("Model slip rate" in Table 1). Correcting for the fault dip (50° on average) increases slip rates by about 0.1 mm/a with respect to the throw rates, largely within the epistemic uncertainties.

The 3D geometry of the master faults has been defined by assuming an average fault dip over the entire seismogenic layer and by constraining the thickness of the seismogenic layer. The average fault dip of the seismogenic faults in the Abruzzo area was fixed at 50° by Boncio et al. (2004a); observation of the L'Aquila 2009 earthquake indicates that this value is a reasonable assumption. The thickness of the seismogenic layer is constrained by well-located instrumental seismicity and thermo-mechanical modelling of the transition depth from brittle-frictional to plastic flow mechanisms (Boncio et al. 2004a, 2009). The seismogenic thickness is not homogeneous across the area, as it is dependent on the heat flow. In the Abruzzo Apennines, the regional surface heat flow decreases from west to east

(from 50–60 mW/m^2 to $\leq$40 mW/m^2, Pasquale et al. 1997). This geothermal heat flux gradient leads to a small (but appreciable) increase in seismogenic thickness from west to east: beneath the master faults (Table 1) it varies from ~13 to ~15 km.

Finally, the seismogenic boxes (SB) reported in Fig. 1 are the projection at the surface of the 3D master faults. Other parameters needed to model these faults in a probabilistic seismic hazard framework, such as the size of the maximum earthquake and its recurrence time, are derived by resorting to the experience of the so-called LASSCI model (see Section 3 below). The geology-based sources proposed here therefore represent a consensus update of previously defined sources, in light of the occurrence of the L'Aquila earthquake, and are limited to the area of main interest for reconstruction and seismic retrofitting after the quake.

3 Response spectra from a layered probabilistic seismic hazard model (LASSCI)

The LASSCI model (LAyered Seismogenic Source model in Central Italy) is an earthquake rupture forecast model developed in the early 2000s (Peruzza and Pace 2002; Pace et al. 2006; Peruzza et al. 2007), based on a schematic representation of different seismogenic sources, formally combined together into a probabilistic seismic hazard assessment, under stationary and time-dependent perspectives.

The LASSCI model contains three separate layers of seismogenic sources, namely the background level (BK), the seismotectonic provinces (SP), and individual faults capable of major earthquakes (seismogenic boxes SB, see Sect. 2). Briefly, the BK layer covers the lower range of magnitude ($2.5 < M \leq 5.4$), and the seismicity rates are obtained by truncated GR relationships for cells centred on a $0.1^\circ \times 0.1^\circ$ grid. The a and b parameters are computed over a search radius of 20 km from the cell's centre. The SP layer returns expected rates of medium-to-large earthquakes following a traditional Cornell-type approach, assuming a homogeneous distribution of earthquakes in space, GR frequency-magnitude relationship, and stationary process with respect to time: this layer includes major events ($M \geq 5.5$) that cannot be assigned to recognised faults (further details on SP characterization can be found in Pace et al. 2006). Finally, for the SB, the expected seismic rates are based on the geometry and kinematics of the faults, and different earthquake recurrence models have been assigned on the basis of historical and instrumental earthquake association.

The original model started being updated in early 2009, when it was formatted for submission to an international validation test (Collaboratory for the Study of Earthquake Predictability CSEP, Schorlemmer et al. 2006, 2009; Italy Testing Region at http://www.cseptesting.org/regions/ita); the changes (Peruzza et al. 2011; Pace et al. 2010) introduced new constraints on fault recurrence times of SB sources, and treat the BK layer as being homogeneous in the SP's.

In this study we used the same layer of BK sources used for CSEP update of the original LASSCI model (details in Pace et al. 2010). Focused on a small area inside the extensional Apennine SP, the contribution of the external SP's, defined as in Pace et al. (2006), is negligible even if formally considered. About SB sources, as previously described in Sect. 2, the fault geometries have been slightly revised after a consensus evaluation and in the light of the 2009 L'Aquila seismic sequence with respect to the original SB's published in Pace et al. (2006). Characteristic magnitude and its mean recurrence time have been recomputed by introducing an error propagation scheme (described in Peruzza et al. 2010, and already used for CSEP update of the model, see details in Peruzza et al. 2011). Their values are given in Table 1. Regarding the model of earthquake recurrence, all faults have been modelled

with an asymmetric Gaussian bell, centred on the maximum magnitude allowed by the fault dimension (characteristic event *s.s.*), and using −3s and +1s for the lower and upper bound, respectively; this asymmetry reduces the critical impact of the highest magnitudes on seismic moment release on the two sides—$M < M_{\max}$; $M > M_{\max}$—of the bell. By scaling properly the occurrences of each magnitude class sampled around $M_{\max}$, the total amount of seismic moment is set equal the seismic moment released by the long-term, maximum event alone, to preserve the seismic moment budget at the source.

About stationarity, or time-dependent assumptions, usually, seismic hazard maps intended for regulation are time-independent, as they portray a long-term average hazard and are not affected by the time of the last earthquake rupture. This attribute makes the maps well suited for use in building codes, where the long-term life of a structure and its resilience to earthquake shaking must be considered. As stated by the International Commission on Earthquake Forecasting for Civil Protection after the L'Aquila earthquake, in its document *Operational Earthquake Forecasting: State of Knowledge and Guidelines for Utilization*[1] exceptions to this rule have been developed for specific areas (e.g. Japan: Earthquake Research Committee 2005; California: Field et al. 2009); these exceptions incorporate time-dependence for the best known faults in the branches of complex logic trees. Even if some of these results were not entered into the national map (e.g. Petersen et al. 2008) local authorities use them for planning (the California Earthquake Authority for earthquake insurance, for example). Developments to existing models are allowing even more complex time dependency.

In Italy, the National Seismic Hazard Maps (Working Group MPS 2004) were last updated in 2004; they are fully time-independent and do not address to individual faults. Despite the provisions given by the law (Ord. 3274/03, available at *zonesismiche.mi.ingv.it/documenti/gazzetta.pdf*), no periodic revision has been proposed at present to include new research results on earthquake faults, crustal deformation and earthquake ground shaking. The national map shows a homogeneous high hazard over a long and wide stripe in the central and southern Apennines; this region is taken as belonging to the same seismogenic zone, and the PGA values and uniform hazard spectra are nearly identical along the entire zone, thus neglecting the details of active faulting knowledge available in this sector of the Apennines.

As the occurrence of a significant earthquake like the 2009 event should be retrospectively used to check the performances of stationary and time-dependent approaches, we explored four different reference models for SB sources, adopting on the structure of the LASSCI framework. The models range from a stationary assumption coherent with the methodological scheme of the national seismic hazard map for regulation (Working Group MPS 2004), to a time-dependent approach applied to SB sources only, computed before and after the April 6 earthquake. The four models are as follows:

1. LADEPOIS: all the individual SB's are treated as Poissonian; this is the hypothesis most similar to the existing seismic hazard map, even if we use individual sources (the SB's) instead of the large seismotectonic zones of ZS9 (Working Group MPS 2004).
2. LADE (LAyered Design Earthquake): we introduced time-dependency by adopting the simplest time-dependent process, namely the renewal process, using the formulation of Brownian passage time (BPT) distributions (Matthews et al. 2002), starting from the

[1] Time-dependent forecasting models have been developed for specific areas in Japan, China, and U.S. National protocols for the operational use of medium-term and short-term forecasts have not yet been established. In California, however, short-term forecasts are updated hourly based on seismicity activity, and operational procedures have been established for the utilization of short-term forecasts www.ias\discretionary-pei.org/downloads/Ex_Sum_v5_THJ9_A4format.pdf.

time elapsed since the last maximum event for each source. The model has been retrospectively applied on March 30, 2009: the Paganica SB (4 in Fig. 2) thereby has an elapsed time equal to 548 years (the last event was on 1461/11/26);

3. LADE1: time-dependency assumptions follow LADE, but with the elapsed time of the Paganica source set to zero, after the April 6 earthquake occurrence; the source is therefore "switched off";
4. LADE2: sources with relatively short elapsed times, having time-dependent earthquake probabilities smaller than those under stationary assumptions, are treated as Poissonian (they are: 3-Pizzoli-Pettino; 4-Paganica; 8-Fucino); the other sources include time-dependency. This approach is precautiounary.

The seismic hazard computations were performed using the well-known code SEISRISK III (Bender and Perkins 1987; LaForge 1996), over an area of about 50 km around L'Aquila, and in particular at four selected sites: L'Aquila, Arischia, San'Eusanio Forconese and Goriano Sicoli (see Fig. 1). In Fig. 2 we reported the expected peak ground acceleration (PGA) values (defined as the acceleration with a 90% of probabilities of not being exceeded in 50 years), obtained by the four recurrence models (LADEPOIS, time-independent forecast; LADE, forecast at 30 March 2009; LADE1, forecast at 30 April 2009; LADE2 forecast at 30 April 2009) and by three different ground motion predictive equations (GMPE), taken from Ambraseys et al. (1996); Sabetta and Pugliese (1996) and Akkar and Bommer (2007).

Some explanation is required with respect to the map prior to the $M = 6.3$ earthquake (Fig. 2a). PGA values exceeding 0.4 g are due to the high earthquake probability assigned to the Paganica source. With an occurrence probability of ~33% for a characteristic event in the 50 years after March 2009, the fictitious recurrence time of an $M \sim 6.3$ event is equal to 124 years. Fictitious recurrence time is computed by solving the equivalence of probabilities given by:

$$P_{\mathrm{Tdep}} = P_{\mathrm{pois}} = 1 - \mathrm{e}^{-t/\mathrm{Tfict}} \tag{1}$$

where P_{Tdep} is the conditional probability obtained by the BPT model, P_{pois} is the poissonian probability, and t is the observation period (50 years).

As the map represents a 475 year return period, for the Paganica SB we can assume a probability of having at least one characteristic event to be about 98% ($P = 1 - \mathrm{e}^{-475/124}$), and therefore the PGA in this SB approaches that of a deterministic scenario. Very similar results have been obtained with the LASSCI fault model updated for the CSEP Italian test, reported by Peruzza et al. 2011. Even if a hazard model cannot be validated by a single earthquake, the results from the LADE model are consistently in agreement with the PGA measurements (Fig. 2a). LADE1 (Fig. 2b) differs from the previous models only in the "absence" of the Paganica characteristic earthquake source (where the probability of occurrence drops to zero after April 6); the PGA level remains high, for the contribution of BK and nearby source in both the northern Abruzzo and Sulmona areas (SB 6). If we tentatively introduce poissonian behaviour for the SB's ruptured in historical time (LADE2, Fig. 2c), the difference is barely noticeable on the map, with only a slight increase of PGA values towards to the south-west. These differences are better shown in Fig. 3, where the single values of PGA for the 4 key municipalities are plotted. In Fig. 2d, where all the sources are assumed to follow a Poisson process in time, a general decrease of the expected PGA is observed, even if the use of well-defined individual seismogenic sources allows computation of PGA values higher than those of the official national hazard map (Working Group MPS 2004, MPS04 in Fig. 3). In the last two frames (Fig. 2e, f), starting from the LADE1 model (Fig. 2b), we have changed the GMPE, following Akkar and Bommer (2007) and Sabetta and Pugliese

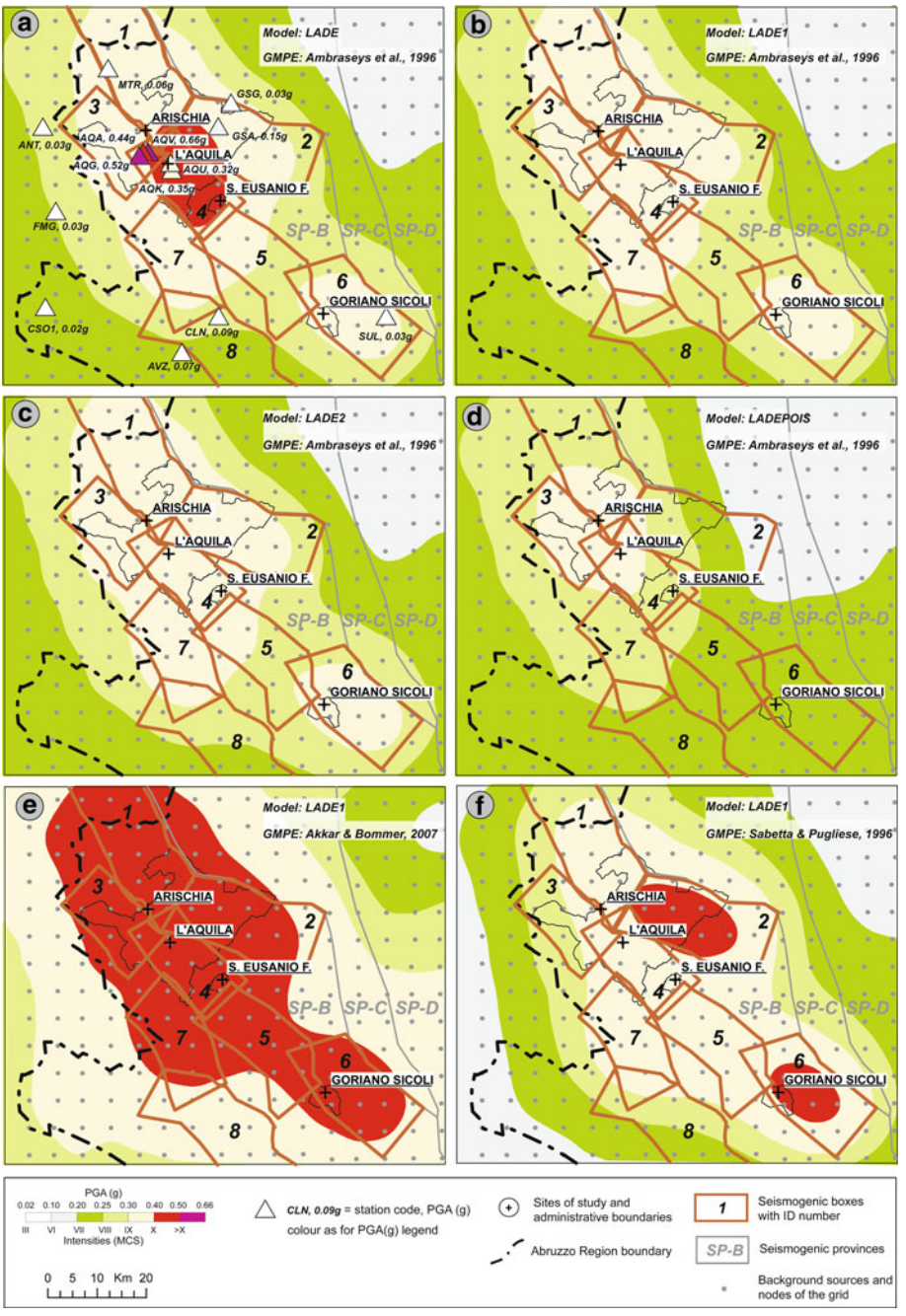

Fig. 2 Seismic hazard maps expressed in terms of PGA with a 50 year 10% exceedance probability. Parts **a–d** show results for the 4 models described in the paper (LADE, forecast at 30 March 2009; LADE1, forecast at 30 April 2009; LADE2 forecast at 30 April 2009; and LADEPOIS, a Poissonian forecast; respectively) and using the Ambraseys et al. (1996) ground motion predictive equation. In part **a** we show also the recorded PGA values for 6th April 2009 (Table 4), and in **e** and **f** we show the results from LADE1 obtained using the Akkar and Bommer (2007) and Sabetta and Pugliese (1996) ground motion predictive equations, respectively. SP-B, SP-C and SP-D are the seismotectonic provinces defined in Pace et al. (2006). The conversion from PGA to MCS is for informative use only (Margottini et al. 1992; Decanini et al. 1995)

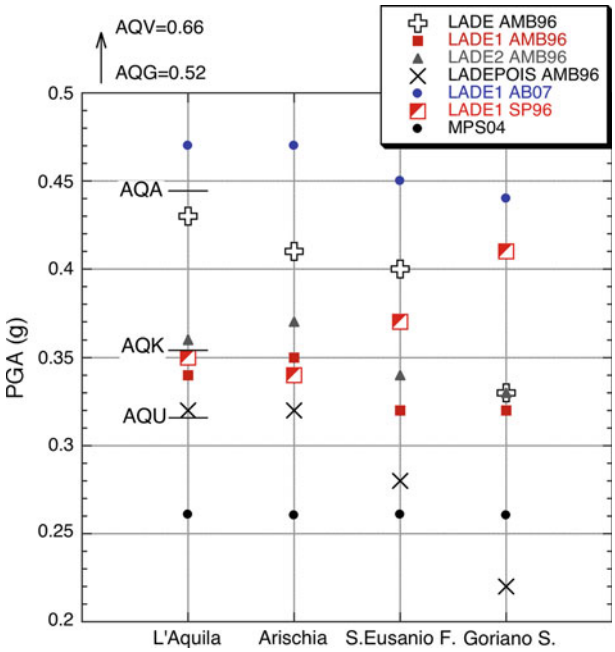

Fig. 3 PGA with a 50 year 10% exceedance probability for the 4 key-municipalities, using the 4 models described in the paper (LADE, LADE1, LADE2 LADEPOIS, respectively) and 3 ground motion predictive equations (GMPEs). The values for the municipalities computed by the Working Group MPS (2004) are also shown as *black dots* (MPS04). PGA recorded on April 6, 2009 in the L'Aquila area are shown with *horizontal traits* (codes explained in Table 4). Abbreviations for GMPEs: AMB96 = Ambraseys et al. (1996); AB07 = Akkar and Bommer (2007); SP96 = Sabetta and Pugliese (1996)

(1996) relationships, respectively. GMPE influences the PGA values, but not the shapes of the most dangerous zones in Abruzzo, which are mainly guided by the source geometries. Even if the Akkar and Bommer relationship produces a large red-coloured spot, the other map shows two well-defined areas of high hazard: one located a few kilometres northeast of L'Aquila (SB 2), and the second on SB 6, near Sulmona. The PGA values obtained for the 4 representative municipalities, are higher in all the tested models than those given by the law (Working Group MPS 2004), and range from 0.3 to 0.5 g with a return period of 475 years (Fig. 3); the use of individual sources makes the PGA more consistent with the values recorded during the L'Aquila earthquake.

For the final choice of a reference model we decided to adopt the LADE1 model, based on the time dependent approach for SB sources that in pre-event conditions (LADE) has demonstrated to be consistent with observations. Time-dependency applied to faults implies the request of higher seismic performances in areas that are considered to be prone to imminent major earthquakes; after such events, or whenever the time dependent approach states that earthquakes are no more or less likely to occur in the next time interval, the seismic demand decreases. In a situation where scientific knowledge is still developing, but with regular upgrading of seismic provisions, this strategy fully satisfies prioritisation schemes based on limited resources (see for example Grant et al. 2007), as long as the time interval considered is tailored to the lifetimes of buildings (conventionally, 50 years). The time-independent component of the LADE1 model layered with BK and SP sources guarantees the

expected ground motion to be as high as the 100% Poisson model (see Fig. 2b, d), and therefore it has been considered as the most appropriate to the aims of the microzoning project.

3.1 Uniform hazard spectra

With the LADE1 model we have calculated uniform hazard spectra (UHS) at 10% exceedance probability in the next 50 years, starting from 30 April 2009 (namely, the return period of the equivalent Poisson process is 475 years) using different GMPE's as follows:

- Sabetta and Pugliese (1996) (SP96). The GMPE is based on the analysis of 95 Italian waveforms, recorded during 17 earthquakes occurring before 1985 with $4.6 \leq M \leq 6.8$ (Ml or Ms). The equation, valid for epicentral distances (R_{epi}), gives the maximum of the two horizontal components of ground motion; it has been slightly corrected for normal fault kinematics following the Bommer et al. (2003) methodology and applied to rock conditions. To apply the required adjustments between different magnitude scales, we used the methodologies described in Ambraseys and Free (1997) and Sabetta et al. (2005).
- Ambraseys et al. (1996) (AMB96). The GMPE is based on the analysis of 422 waveforms of 157 earthquakes in Europe and adjacent regions. The equation is formulated for the "Joyner and Boore" distance (R_{jb}) defined as the closest distance to the surface projection of the fault rupture, and returns the maximum value of the horizontal components of ground motion. In order to apply the correction between R_{jb} and R_{epi} and between geometrical mean and maximum value of the horizontal components, we used the methodologies described by Scherbaum et al. (2004) and Sabetta et al. (2005).
- Akkar and Bommer (2007) (AB07). The GMPE is based on the analysis of 532 waveforms, recorded during 132 European earthquakes, more than half of which occurred in Italy, with $5.0 \leq M \leq 7.6 (M_w)$. The equation uses the R_{jb} distance, returns the geometrical mean of the horizontal components and is based on normal faulting and rock conditions.

The obtained UHS for the 4 sites are very similar to each other. In Fig. 4 we compared the calculated UHS of L'Aquila with that of the NTC-08 regulation (Norme Tecniche di Costruzione; Decreto 2008) obtained from the PGA values of the national seismic hazard assessments (Working Group MPS 2004; http://esse1.mi.ingv.it/d3.html), expected for L'Aquila (these values are very similar to those for the other three municipalities). It is clear that the computed spectra are considerably higher than those for NTC-08. We attribute this result to the effect of individual seismogenic sources, which have more detailed geometry than the zones of the national hazard model, and to the application of time-dependent approach.

The GMPE choice cannot disregard the site-to-source metrics used by the hazard software, or how the software handles uncertainties. In particular, the 2D or 3D geometrical definition of the sources, and consistent distance settings, are critical parameters in terms of near field seismic hazard evaluations. To maximize the potential for comparison between our results and previous studies (MPS04, Working Group MPS 2004; LASSCI, Pace et al. 2006), we adopted the same software (SEISRISKIII, Bender and Perkins 1987) that utilizes bi-dimensional areal sources or faults represented by surface traces. With seismogenic sources represented by the surface projection of the 3D active normal faults, the definition of site-to-source distance is, as a first approximation, equivalent to R_{epi}. The AB07 relationships utilize R_{jb} and therefore need some corrections; the SP96 equations use R_{epi} and are consequently more suitable in this framework. The AMB96 relationships, also used in MPS04, yielded problems in the

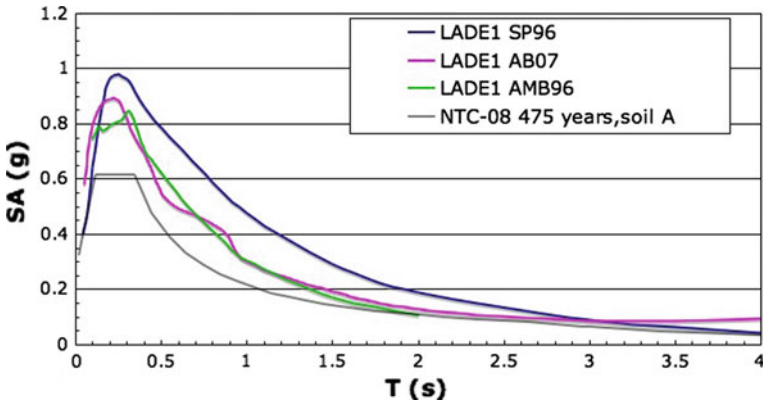

Fig. 4 Acceleration response spectra, at 5% damping and for rock sites. LADE1 is the chosen time-dependent model, with forecast at 30 April 2009 (details in the text); abbreviations for GMPEs: AMB96 = Ambraseys et al. (1996); AB07 = Akkar and Bommer (2007); SP96 = Sabetta and Pugliese (1996); NTC-08 475 years; soil A = Norme Tecniche di Costruzione (Decreto 2008) obtained from the PGA values of the national seismic hazard assessments (Working Group MPS 2004)

very near field, and the UHS show anomalous patterns at low periods due to the contribution to hazard given by the background layer (Fig. 4).

Another troubleshooting issue in the GMPE's is the magnitude-dependent uncertainty. For example, the pronounced bump in the AB07 curve of Fig. 4 is due to this dependency: in any case, there are controversial opinions regarding the use of $\sigma = f(M)$ (e.g. Musson 2009).

In Fig. 5 we reported the variation of σ versus the spectral ordinates for three classes of magnitude compared with the σ of AMB96; it is clear the peak of σ is at around 0.9 s. Moreover the AB07 equation shows problems for periods greater then 3 s, where the curve is flat without the expected $1/T^2$ decreasing (Fig. 4).

In conclusion, for the above reasons, we chose the SP96 GMPE for both the deterministic and probabilistic approaches.

3.2 Disaggregation

We conducted a disaggregation analysis, with a modified version of the SEISRISKIII code (LaForge 1996), in order to separate the contributions of each individual source to the total hazard and to define magnitude/distance pairs useful for the deterministic approach. Two disaggregation schemes for regional seismic hazard are used in the literature. The first method, suitable when sources are symmetrically distributed around the site, separates the contributions into a limited number of ranges of annular distance, magnitude and ground-motion level (McGuire 1995). The second method, named "geographic disaggregation" of hazard, separates the contributions into causative sources, magnitude, and ground-motion level (Bazzurro and Cornell 1999; Harmsen and Frankel 2001). Following the methodological scheme of Pace et al. (2008), we used this latter method only for the SB layer, in order to identify the individual seismogenic sources which dominate the hazard.

Figure 6 shows the percentage contribution to hazard of the sources from different peak ground acceleration classes. The model assumptions are critical in defining which source dominates the hazard; we represent in Fig. 6 the disaggregation for the LADE1 model,

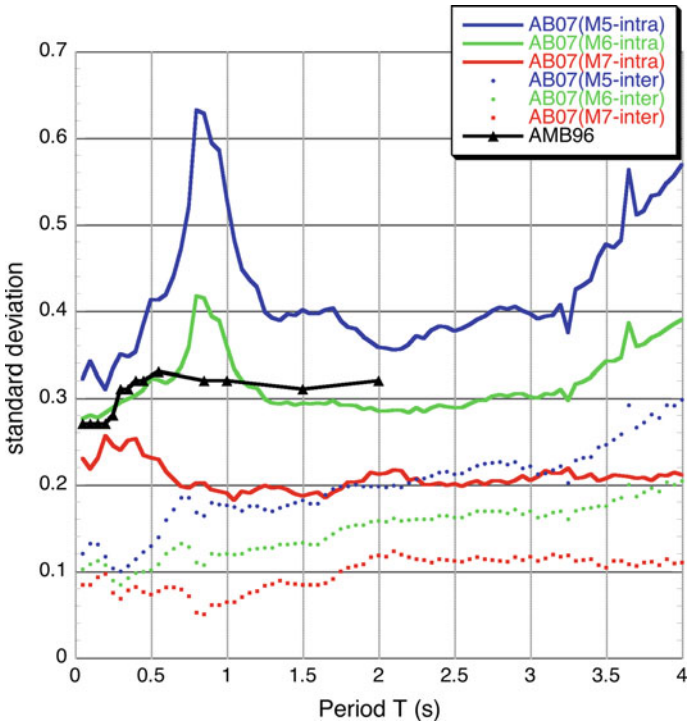

Fig. 5 Variations of the standard deviation versus spectral periods. *Black triangles* (AMB96) represent the Ambraseys et al. (1996) standard deviation, that is not magnitude-dependent. *Coloured lines* are the magnitude-dependent errors from Akkar and Bommer (2007) GMPE, for the intra- and inter-events components at three magnitude values. Note the similarity of AB07 intra-events error at $M = 6$ with AMB96, except the peak of standard deviation at 0.85 s. Note also the sub-parallel behaviour of inter and intra-event variability

which is our "consensus" model. The attenuation relationship appears to impact on the absolute value of shaking instead of the relative contributions of single sources. For this analysis we used the SP96 GMPE. The sources that provide the main contribution to hazard in the 4 selected municipalities, in relation to the selected hazard level (10% of exceedence in 50 years) are the 2-Gran Sasso for *L'Aquila*; the 1-Gorzano for *Arischia*; the 6-Sulmona for *Goriano Sicoli*; and the 2-Gran Sasso for *Sant'Eusanio Forconese* (see Fig. 3, Table 2). The characteristic earthquake for all these sources is estimated to have an expected magnitude around $M_w \sim 6.6$–6.7. This analysis demonstrates that even if the UHS are very similar, the dominating source is different for each locality, and different choices of reference earthquakes could be invoked. The estimation of the site-source distance also requires, implicitly, the definition of a position for the nucleation of rupture on the fault plane: this is particularly important when the source size is comparable to the site-source distance. Table 2 summarizes the magnitude/distance pairs of earthquakes having the highest contributions to the hazard at the four studied sites. We computed two different site-to-source distances: the "Joyner and Boore" distances (R_{jb} in Table 2), and the epicentral distances (R_{epi} in Table 2), obtained by converting the R_{jb} into epicentral distances using the formulation of Scherbaum et al. (2004). For all the 4 municipalities, R_{jb} is less than 7 km, but introducing R_{epi} yielded values ranging between 5 and 14 km.

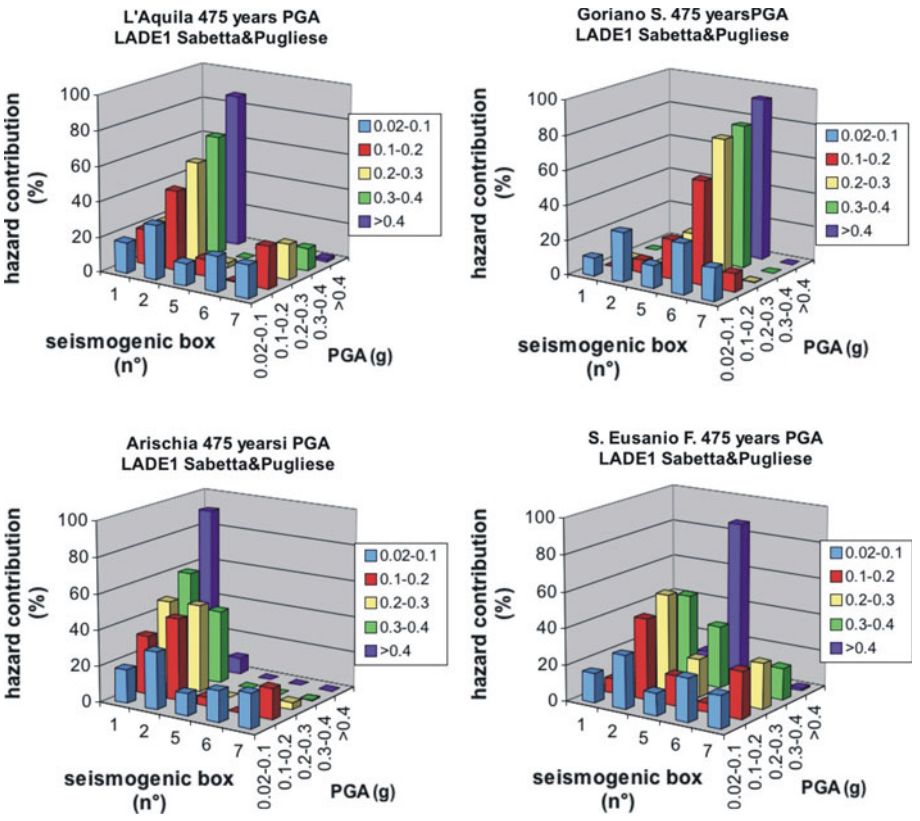

Fig. 6 Disaggregation analysis obtained with the LADE1 model and Sabetta and Pugliese (1996) attenuation relationship. In each 3D diagram we show the contribution of each individual seismogenic source (SB) to the total hazard for 5 classes of PGA, for the four key municipalities: L'Aquila, Goriano Sicoli, Arischia and Sant'Eusanio Forconese

Table 2 Contribution of each individual source to the total hazard for the two highest classes of PGA, and associated magnitude/distance pairs

Site	PGA classes	Seismogenic source	Hazard contribution (%)	M_w	R_{jb} (km)	R_{epi} (km)
L'Aquila	0.30–0.38	(2) Gran sasso	67	6.7	2	9.1
	0.40–0.60		87			
Arischia	0.30–0.38	(1) Gorzano	59	6.7	0	4.9
	0.40–0.60		91			
Sant'Eusanio Forconese	0.30–0.38	(2) Gran sasso	48	6.7	6.3	13.8
	0.40–0.60	(5) M. Aterno V.	87	6.7	1.6	8.7
Goriano Sicoli	0.30–0.38	(6) Sulmona	82	6.6	0	6.3
	0.40–0.60		93			

The model used is the LADE1 with the SP96 GMPE. M_w is the characteristic moment magnitude; R_{jb} the "Joiner & Boore" distance; R_{epi} the epicentral distance computed following Scherbaum et al. (2004) starting from R_{jb}

4 M–D pairs from probabilistic analysis of site historical intensities

Another analysis was performed on macroseismic data (experienced historical intensities), for selecting different magnitude/distance pairs representative of seismic hazard at the four sites considered. These results are useful for the deterministic approach, but require specific procedures to manage the peculiar properties of intensity data (that are ordinal, discrete and defined over a finite non-metric scale) in the frame of a coherent probabilistic approach. A procedure of this kind was first proposed by Magri et al. (1994) and progressively improved (for the most recent developments, see Albarello and Mucciarelli 2002; D'Amico and Albarello 2008).and applied for seismic hazard assessment in Italy can be found in Azzaro et al. (1999, 2008); Mucciarelli et al. (2000, 2008); Albarello et al. (2002); D'Amico and Albarello (2003) and Gomez Capera et al. (2010). The bulk of this approach is in the computation of the "expected" number N of earthquakes that in a time window of dimensions equal to the exposure time have shaken the site under study with intensity larger or equal to an intensity threshold I_s. This number is provided by the relationship

$$\nu\,(I_s) = \sum_{l=1}^{N} P_l(I_s) \tag{2}$$

where the N is the number of earthquakes occurring during the considered time window and $P_l(I_s)$ is the probability that the lth earthquake affected the site with an intensity equal or greater than I_s. In fact, a probabilistic evaluation is required to account for uncertainty relative to ill-defined intensities (see D'Amico and Albarello 2008 for details). Thus, the role of a single lth event in the determination of hazard at the intensity threshold I_s at the site under study, ultimately depends on the value of $P_l(I_s)$ that can be considered as a "weight" of the single event in the local hazard.In this formalization one can identify those single events that contribute most weight to computed hazard at the intensity threshold I_{ref}. In the present study, I_{ref} values relative to an exposure time of 50 years and an exceedance probability of 10%, have been computed for the four sites of Arischia, L'Aquila, S'Eusanio Forconese and Goriano Sicoli. Site seismic histories used for computations have been taken from the historical earthquakes described in Section 1 (see Fig. 1 for epicentral location) by using the Italian database of macroseismic intensities (DBMI04, http://emidius.mi.ingv.it/DBMI04). An I_{ref} value of IX MCS was obtained for Arischia, L'Aquila and S.Eusanio Forconese, while an I_{ref} of VIII MCS was obtained for Goriano Sicoli. By taking these values as references, earthquakes with $P_l(I_s)$ values larger than 0 have been selected for each considered site. Relevant epicentral distances and macroseismic magnitudes (M_w compatible) were deduced for each of these events from the epicentral catalogue CPTI04. Thus, for each site, these values were binned in classes of epicentral distances (5 km intervals) and magnitude (0.5 units intervals). The weights relative to each earthquake were summed in the relevant distance/magnitude cell to provide a type of "disaggregation scheme" presented in Table 3. Being the representation of actual earthquakes, the distribution is multimodal, but some clear "polarizations" are shown. On the basis of these data, one representative magnitude/distance pair was selected for each site, by considering a "cautious" perspective (i.e, the lower bound of the distance bin and the upper bound of the magnitude bin were selected for the relevant maximum). In this way, the pairs (7 M_w, 10 km), (6.5 M_w, 10 km), (6.5 M_w, 5 km) and (6.5 M_w, 10 km) were selected for Arischia, L'Aquila, S.Eusanio Forconese and Goriano Sicoli respectively (see Historical intensities columns in Table 5). One can note that these results are similar to the ones obtained by the disaggregation analysis with the non-Poissonian seismotectonic approach (previous chapter), but very different from the values provided by the standard disaggregation scheme

Table 3 Disaggregation scheme obtained from the probabilistic site-approach to macroseismic intensities in the four analyzed sites

Arischia							
dis/mw	4.25	4.75	5.25	5.75	6.25	6.75	7.25
5	0.00	0.00	0.00	0.00	0.00	0.00	0.00
15	0.00	0.00	0.00	0.00	0.00	0.41	0.00
25	0.00	0.00	0.00	0.00	0.50	0.00	0.00
35	0.00	0.00	0.00	0.00	0.00	0.05	0.00
45	0.00	0.00	0.00	0.02	0.00	0.00	0.00
55	0.00	0.00	0.00	0.00	0.00	0.00	0.00
65	0.00	0.00	0.00	0.00	0.00	0.00	0.00
75	0.00	0.00	0.00	0.00	0.00	0.01	0.00
85	0.00	0.00	0.00	0.00	0.00	0.00	0.00
95	0.00	0.00	0.00	0.00	0.00	0.00	0.00
105	0.00	0.00	0.00	0.00	0.00	0.00	0.00
115	0.00	0.00	0.00	0.00	0.00	0.00	0.00
125	0.00	0.00	0.00	0.00	0.00	0.00	0.00

S.Eusanio Forconese							
dis/mw	4.25	4.75	5.25	5.75	6.25	6.75	7.25
5	0.00	0.00	0.00	0.12	0.31	0.00	0.00
15	0.00	0.00	0.00	0.00	0.30	0.00	0.00
25	0.00	0.00	0.00	0.00	0.00	0.00	0.00
35	0.00	0.00	0.00	0.00	0.00	0.22	0.00
45	0.00	0.00	0.00	0.00	0.02	0.00	0.00
55	0.00	0.00	0.00	0.00	0.00	0.03	0.00
65	0.00	0.00	0.00	0.00	0.00	0.00	0.00
75	0.00	0.00	0.00	0.00	0.00	0.00	0.00
85	0.00	0.00	0.00	0.00	0.00	0.00	0.00
95	0.00	0.00	0.00	0.00	0.00	0.00	0.00
105	0.00	0.00	0.00	0.00	0.00	0.00	0.00
115	0.00	0.00	0.00	0.00	0.00	0.00	0.00
125	0.00	0.00	0.00	0.00	0.00	0.00	0.00

L'Aquila							
dis/mw	4.25	4.75	5.25	5.75	6.25	6.75	7.25
5	0.00	0.01	0.00	0.00	0.00	0.00	0.00
15	0.00	0.00	0.00	0.00	0.32	0.00	0.00
25	0.00	0.00	0.00	0.00	0.32	0.32	0.00
35	0.00	0.00	0.00	0.00	0.00	0.00	0.00
45	0.00	0.00	0.00	0.00	0.00	0.00	0.00
55	0.00	0.00	0.00	0.01	0.00	0.00	0.00
65	0.00	0.00	0.00	0.00	0.00	0.00	0.00
75	0.00	0.00	0.00	0.00	0.00	0.00	0.00
85	0.00	0.00	0.00	0.00	0.00	0.00	0.00
95	0.00	0.00	0.00	0.00	0.00	0.00	0.00
105	0.00	0.00	0.00	0.00	0.00	0.00	0.00
115	0.00	0.00	0.00	0.00	0.00	0.00	0.00
125	0.00	0.00	0.00	0.00	0.00	0.00	0.00

Goriano Sicoli							
dis/mw	4.25	4.75	5.25	5.75	6.25	6.75	7.25
5	0.00	0.00	0.00	0.00	0.00	0.00	0.00
15	0.00	0.00	0.00	0.00	0.17	0.00	0.00
25	0.00	0.00	0.00	0.01	0.00	0.33	0.00
35	0.00	0.00	0.00	0.00	0.28	0.00	0.00
45	0.00	0.00	0.00	0.00	0.00	0.00	0.00
55	0.00	0.00	0.00	0.00	0.02	0.00	0.00
65	0.00	0.00	0.00	0.00	0.00	0.04	0.00
75	0.00	0.00	0.00	0.00	0.00	0.08	0.00
85	0.00	0.00	0.00	0.00	0.00	0.01	0.00
95	0.00	0.00	0.00	0.00	0.00	0.00	0.00
105	0.00	0.00	0.00	0.00	0.00	0.00	0.00
115	0.00	0.00	0.00	0.00	0.00	0.03	0.00
125	0.00	0.00	0.00	0.00	0.00	0.00	0.00

The tables indicate the overall contribution of events that have occurred within bins of epicentral distance (in km) and magnitude (M_w equivalent): the number in headers indicates the bin midpoint. Relative maxima are highlighted

performed on MPS04 results for the considered sites (see data reported in http://esse1-gis.mi.ingv.it/s1_en.php); the pairs obtained here result much stronger. We argue that the comparison of disaggregation outcomes from macroseismic approach described above with those provided by the National Seismic Hazard Map is methodologically acceptable. In fact, both approaches share the same main assumption of a stationary seismogenic process. This implies that in both cases, past seismicity is considered as representative of the future. In both cases, "representative" events are chosen as those that contribute most weight to the computed local seismic hazard at the same exposure time (50 years) and exceedance probability (10%).

The fact that in one case (macroseismic analysis) magnitude/distance pairs correspond to "true" earthquakes and that in the other case a "virtual" event is obtained, only arises from the standard approach, where "distributing" events over large seismogenic structures prevents tracing single contributions. This, however, does not change the interpretation of results provided by the considered approaches that must be seen as completely equivalent.

On the other hand, the strong differences in outcomes resulting from the considered approaches should be explained, since both these approaches ultimately share the same

seismic databases. A possible interpretation relies on the different use of this information: in one case (the standard approach) seismicity is artificially distributed over large areas (seismogenic regions) while in the other case (macroseismic) locally-felt effects and actual epicenters are considered. This is responsible for a marked difference in the level of "polarization" of seismic hazard between the two approaches (see Mucciarelli et al. 2008 for a detailed discussion of this aspect).

If one considers the low level of precision for the epicentral location of historical events, the M–D pairs deduced from the macroseismic approach result in good agreement with those provided by the time-dependent analysis. This agreement is also impressive (and to some extent surprising) because, in the macroseismic approach, no geological information (fundamental in the time-dependent fault-based model) was considered. One can interpret this convergence as an indirect validation of theoretical estimates provided by the LASSCI model with historical records.

In conclusion, the disaggregation results obtained in this study suggest M–D pairs to be considered in the selection of a deterministic design earthquake. By taking into account relevant uncertainties in distance metric (location) and magnitude, and the relatively small differences in outcomes obtained by the two approaches for the four towns, one single representative average M–D pair can be chosen for all sites. This pair has the characteristic M_w 6.7 and R_{epi} =10 km.

5 Strong motion recordings of the L'Aquila earthquake and characterization of a compatible seismic input

L'Aquila seismic sequence provided strong motion recordings of major earthquakes nearby the causative source, which are not common in waveform databases. The Italian Accelerometric Archive (http://itaca.mi.ingv.it/ItacaNet/), for example reports only 6 time histories form $M > 6.0$ events at $R_{\text{epi}} < 12$ km, and 5 seismograms are those of the April 6, 2009 main event. It is therefore mandatory to take into consideration these response spectra in the definition of a deterministic seismic input.

Fifty-eight of the approximately 300 digital strong-motion stations of the Italian Strong Motion Network (RAN, see Gorini et al. 2010 for details on the network) managed by the Italian Department of Civil Protection (DPC) were triggered by the main shock of April 6, 2009. In addition, the INGV broadband station AQU, located close to the L'Aquila centre, was also equipped with an accelerometer that recorded the main shock. Figure 7 shows the locations of the strong motion stations at a distance less than 6 km from the epicentre, together with the surface projection of the ruptured fault. All these stations fall inside the hanging wall of the fault surface projection (R_{jb} distance equal to zero) and, apart from AQU and AQK, correspond to the "Valle dell'Aterno" array. Only two of the eight stations, AQF and AQP (red triangles in Fig. 7) did not record the main shock due to low power supply of the solar panels

Strong-motion parameters of the main shock for the 15 recordings with PGA > 25 cm/s^2 are reported in Table 4 (see Akinci et al. 2009 for details). The first five columns report the station name, station code, Joyner-Boore distance (R_{jb}), epicentral distance (R_{epi}), and station soil condition described according to the Eurocode EC8 classification, derived from boreholes Vs measurements collected after the earthquake (http://itaca.mi.ingv.it/ItacaNet). The strong-motion parameters, for the largest value of the horizontal components, are PGA, PGV, Arias Intensity (Arias 1970), Housner Intensity (Housner 1952) and two significant durations according to the definition of Vanmarcke (Vanmarcke and Lai 1980) and Trifunac

Table 4 Strong motion parameters for the largest horizontal component of the 15 recordings with PGA> 25 cm/s^2: stations are sorted in descending order of PGA

Station name	Station code	Rjb distance (km)	Epic. distance (km)	EC8 site class	PGA (cm/s2)	PGV (cm/s)	Arias Intensity (cm/s)	Housner Intensity (cm)	Duration Vanm (s)	Duration Trif (s)
V. Aterno–Centro Valle	AQV	0	4.9	B	646.1	42.83	285.7	94.5	3.1	7.8
V. Aterno–Colle Grilli	AQG	0	4.4	B	506.9	35.54	137.0	92.2	2.9	8.6
V. Aterno–f. Aterno	AQA	0	4.6	B	435.6	32.03	175.0	86.1	4.8	7.7
Aquila parcheggio	AQK	0	5.6	B	347.2	36.21	128.9	68.1	4.8	15.5
Aquila Castello (INGV)	AQU	0	5.8	B	309.5	35.00	71.0	78.0	5.0	7.5
Gran Sasso (Assergi)	GSA	8.6	18.0	A	148.2	9.84	44.0	17.8	3.6	8.9
Celano	CLN	20.0	31.6	A	89.1	6.64	9.5	14.3	3.9	7.7
Avezzano	AVZ	25.1	34.9	C	67.7	11.28	9.7	27.3	6.5	19.0
Ortucchio	ORC	37.3	49.3	A	64.2	5.86	7.4	17.8	5.2	12.3
Montereale	MTR	15.9	22.4	B	61.6	3.53	5.8	9.7	6.9	15.4
Sulmona	SUL	43.4	56.4	A	33.6	3.73	1.0	7.0	6.7	17.7
Chieti	CHT	52.2	67.0	B	29.4	7.91	3.8	10.3	9.5	31.7
Gran Sasso (Lab. INFN)	GSG	13.7	22.6	A	29.4	3.04	0.9	4.9	4.9	11.7
Famignano	FMG	16.6	19.3	A	26.3	2.61	1.2	6.4	8.4	21.0
Antrodoco	ANT	19.3	23.0	A	26.0	2.47	1.8	6.9	8.9	22.7

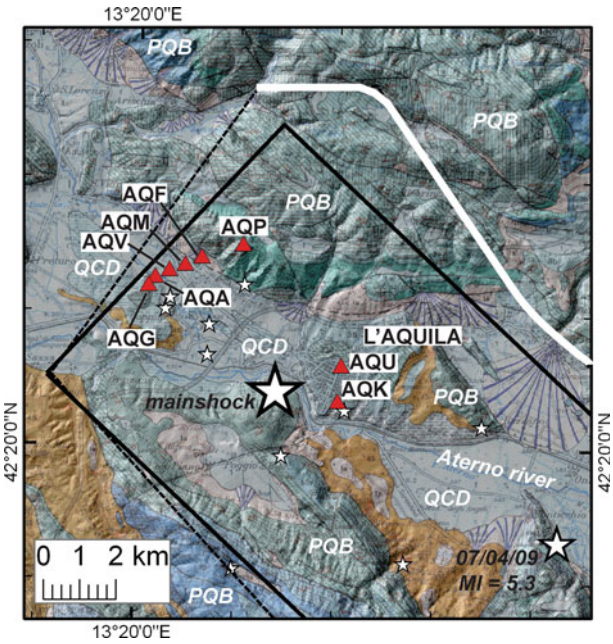

Fig. 7 Map of the strong motion stations (*red triangles* parameters in Table 4) in the very near field. RAN stations are accelerometric stations managed by the Italian Department of Civil Protection, AQU is the accelerometer coupled to the broadband INGV station that saturated during the main shock. All the recording sites are located on the surface projection of the ruptured fault (*solid black line* Atzori et al. 2009 from inversion of DInSAR data; *dashed black line* and *solid white line* geology-based seismogenic source and its master fault, respectively, from this study). Epicentral locations (*white stars*) are taken from Chiarabba et al. 2009. Geologic map is taken from Vezzani and Ghisetti (1998). *PQB* pre Quaternary bedrock, *QCD* Quaternary continental deposits

(Trifunac and Brady 1975). It should be noted that the high value of PGA (>0.3 g) for all the stations at zero distance from the fault and the very short duration (2–5 s according to the Vanmarcke definition that does not overestimate the "strong phase" duration as the Trifunac definition does) are compatible with the high frequency content of the recordings confirmed by the response spectra analysis.

Data recorded at stations of the "Valle dell'Aterno" array are of particular interest as they are close to heavily damaged areas (Pettino), whereas AQK and AQU are in the immediate vicinity of L'Aquila. Brief descriptions of the station site conditions are as follows (Çelebi et al. 2009, http://itaca.mi.ingv.it/ItacaNet):

- Station AQG has a velocity profile obtained from down-hole measurements with a V_{S30} of 685 m/s, a natural frequency $f_0 = 5.7$ Hz from H/V microtremors, and may experience topographical effects as it sits on a slope of weathered calcareous rocks.
- Station AQV is characterized by a velocity profile with a V_{S30} of 474 m/s, a natural frequency fo = 3.0 Hz from H/V microtremors, and shows a Vs inversion between 20 and 30 m whereby Vs decreases by up to 300 m/s.
- Station AQA is similar to AQV but with thinner Holocene alluvial deposits and a velocity profile with a V_{S30} of 552 m/s.
- Station AQK has a velocity profile with a V_{S30} of 717 m/s. It is located behind the L'Aquila Bus Station building on top of a retaining wall, and all the available H/V ratios

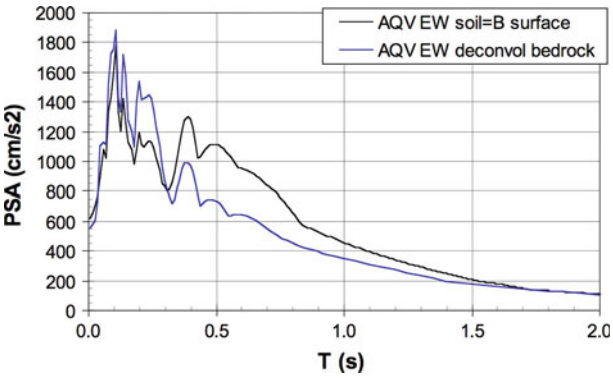

Fig. 8 Acceleration response spectra, at 5% damping, of the EW component at station AQV as recorded at the surface (*black line*) and deconvoluted at the bedrock (*blue line*) using SHAKE software

show a remarkable amplification at 0.6 Hz as also demonstrated by De Luca et al. (2005) using weak motion and ambient noise data.

- Station AQU is located in an underground vault beneath the north tower of the L'Aquila Castle at the northeastern corner of the old city of L'Aquila and lies on the same kind of soil as that described for AQK.

Using the velocity profile for station AQV, a specific study was implemented for the characterization of bedrock ground motion compatible with the main shock recordings. The deconvolution analysis from the surface to the bedrock was performed with the SHAKE software package (Schnabel et al. 1972). Results are reported in Fig. 8, and reveal that the alluvial deposits under station AQV amplify the bedrock motion only at periods higher than 0.3 s whereas, due to the non-linear response and to the velocity inversion, they dampen motion at shorter periods. The results of the deconvolution analysis were confirmed by local amplification studies carried out at stations AQK and AQU. Those stations, if subjected to the above-mentioned bedrock motion, show a significant reduction of the motion at the surface due to the filtering effects of the lacustrine sediments, confirming the relatively lower acceleration values recorded at AQK and AQU.

Nonetheless potential source and site effects observed in the L'Aquila area, the choice of using a deterministic application of GMPE instead of the recorded ground motions demonstrated its adequacy. It is illustrated in Fig. 9, which shows the EW component of the acceleration response spectra at 5% damping for the stations AQV, AQG, AQK and AQU (Fig. 9a), and two European earthquakes records (from the European Strong Motion Database; www.isesd.hi.is) with comparable M–D pairs (Fig. 9b), together with the response spectrum derived from the attenuation relationship SP96 (Sabetta and Pugliese 1996) for the same magnitude and distance from the main shock of L'Aquila sequence. Station AQV yields the highest values at short periods, reaching about 1.8 g at 0.1 seconds, while AQK, with more moderate values at short periods, also exhibits large values at long periods in agreement with the site amplification at 0.6 Hz (1.66 s) revealed by the H/V ratios and discussed in the literature (De Luca et al. 2005). The response spectra indicate that the shaking is particularly strong at periods (0.1–0.5 s) that are typical of the 1–5 story buildings, both in L'Aquila and throughout the region. It is interesting to note that the SP96 spectrum, with lower median values than those of the recorded spectra, lies well inside the ± 1 sigma bounds even for the highest spectral values, both for the L'Aquila records

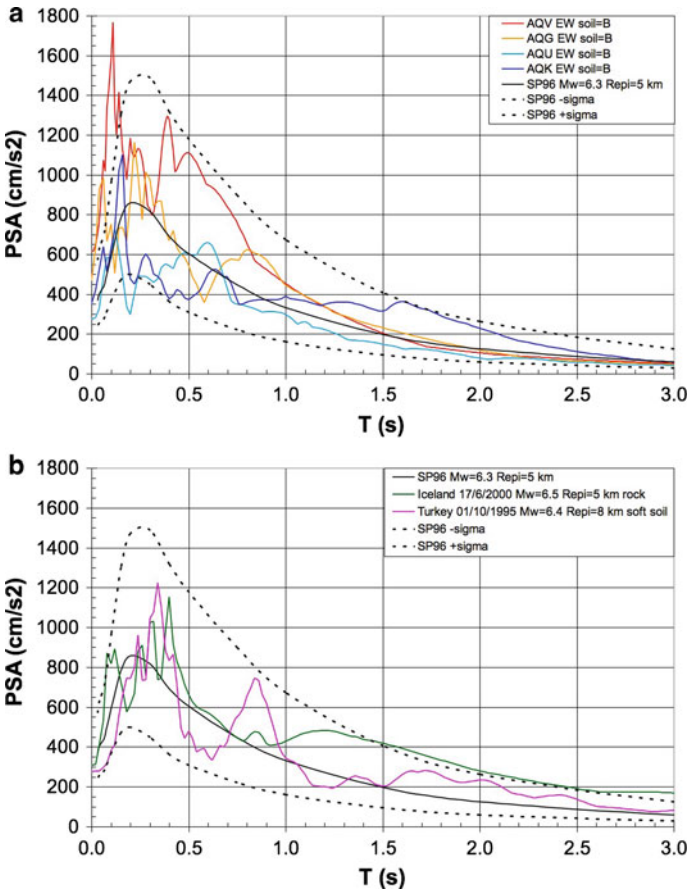

Fig. 9 The *couloured lines* are the acceleration response spectra, at 5% damping, for the stations closest to the epicentre (Fig. 9a) and for two additional records from the European Strong Motion Database (www.isesd.hi.is; Fig. 9b); the *black lines* are the deterministic response spectrum obtained with the attenuation relationship of Sabetta and Pugliese (SP96, stiff soil condition) of an earthquake with magnitude/distance similar to the L'Aquila main shock, with its confidence limits

and European records with comparable M–D pairs, only with the exception of very short periods.

It is therefore appropriate as possible characterization of the seismic input to be expected in L'Aquila area from future earthquakes, the use of SP96 that, like all the GMPEs, makes use of large statistical samples rather than single earthquake recordings.

6 Conclusions

In late 2009, a team of about 150 researchers and experts performed seismic microzoning activities aimed at seismic reconstruction in Abruzzo. We presented in this paper the analyses established in the framework of Task 6, *Definition of Design Earthquakes for Numerical*

Table 5 Magnitude-Distance pairs obtained from different probabilistic approaches: non-Poissonian layered LADE1 model; stationary site-approach to historical intensities; mean values given by disaggregation analysis of the regulation map MPS04 (Working Group MPS 2004)

	Disaggregation LADE1		Historical intensities		MPS04 (mean values)	
	M_w	Repi	M_w	Repi	M_w	Repi
Arischia	6.7	4.9	7.0	10	5.7	7.9
L'Aquila	6.7	9.1	6.5	10	5.7	7.9
Sant'Eusanio Forconese	6.7	13.8	6.5	5	5.7	8
Goriano Sicoli	6.6	6.3	6.5	10	5.7	7.9

Simulations. Using both probabilistic and deterministic approaches, we defined response spectra in four selected localities that can be used as seismic input.

A geology-based seismogenic source model has been updated to generate earthquake rupture forecasts and probabilistic seismic hazard assessments. We explored various models introducing the time-dependency of individual sources of major earthquakes located in the study area; the LADE1 model we adopted uses a renewal BPT process that gives conditional probabilities as a function of the time elapsed since the last major event for each source. The Paganica SB (4 in Fig. 1) is "switched off" after the April 6 earthquake event; background sources and seismotectonic provinces (outside of the study area) taken from previous studies account for the occurrence of minor and far earthquakes, under traditional, stationary assumptions. PGA values obtained by our analyses (Figs. 2, 3) are significantly higher than those given by the 2004 national regulation map (Working Group MPS 2004); the PGA patterns are controlled by the source model, but their absolute values depend on different behaviours of the attenuation relationships, especially in the near-field. When comparing this approach with other methods, we did not combine the results in branches of a logic tree; uniform hazard spectra are instead computed according to the LADE1 model and the different attenuation relationships (Fig. 4), and compared with observations and building code spectra, as discussed in the paper.

In order to define the magnitude/distance pairs representative of seismic hazard at the four selected sites, we conducted disaggregation analyses both from the time-dependent probabilistic seismic hazard assessment (Fig. 6, Table 2) and from the probabilistic site-approach, based on the historical macroseismic data (Table 3). The average values of magnitude and distance resulting from both the methods are consistent, providing values of about 6.7 for magnitude, and about 10 km for epicentral distance. We argued that small variations of M and R_{epi} shown in Tables 2 and 5 for the four sites analysed do not significantly change the resulting response spectra.

As the national building code prescriptions have to be taken into consideration, and because this new study provides additional, more cautious results for seismic designers and planners, we decided to select response spectra obtained by a selection of different methodologies, and we propose these as end-member inputs to be used for the numerical simulation of the seismic microzoning of the L'Aquila area. They are as follows (see Fig. 10):

1. The uniform hazard spectrum of the Italian building code NTC-08 (Decreto 2008) corresponding to the four sites considered as representative of the study area. These parameters are identical in all the four sites, because they all belong to the same source, modelled in MPS04 by a long stripe of uniformly distributed seismicity. This represents the official

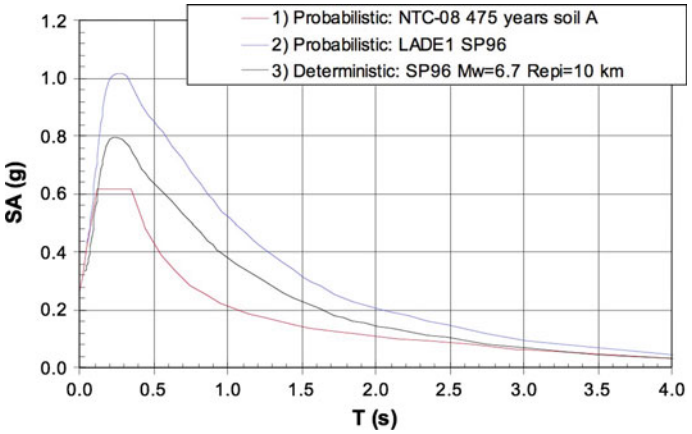

Fig. 10 Acceleration response spectra, at 5% damping, for rock sites selected as input for the seismic microzoning

prescriptive reference of the Italian regulations for the study area, and provides a lower bound for the expected seismicity.

2. A probabilistic uniform hazard spectrum obtained by the LADE1 source model, and the SP96 GMPE. As discussed above, even if the spectra are still practically the same at all the reference sites, they pertain to different individual geology-based sources. This spectrum gives an upper bound, reaching a maximum spectral value of about 1 g at 0.25 s.
3. A deterministic spectrum obtained from the SP96 GMPE for a magnitude-distance pair (M_w 6.7, $R_{\text{epi}} = 10$ km) derived from the two disaggregation analyses described in the paper. The pairs at each site refer to a different dominant event that should be easily identified (in terms of the corresponding fault and historical earthquake) in the disaggregation analyses. The deterministic spectrum gives intermediate values ranging from 0.35 g at 0 s, to 0.8 g at 0.25 s and 0.4 g at 1 s.

In conclusion, we believe that the above-mentioned spectra are the most appropriate to be used as input for the numerical simulation of the seismic microzoning of the L'Aquila area. Time-dependency applied to faults implies the request of higher seismic performances in areas that are considered to be prone to imminent major earthquakes. By introducing time-dependency we are able to tune the Abruzzo seismic hazard estimates to the new results released by the international scientific community, and adopted by some local authorities (California, Japan) for specific purposes. The agreement in terms of magnitude-distance pair identification between the non-Poissonian seismotectonic approach and stationary macroseismic site-approach is impressive; we interpret this convergence as an indirect validation of theoretical estimates provided by a layered, geology-based model with historical records.

As scientific knowledge grows faster after a devastating earthquake, and because regular upgrading of seismic provisions is anticipated, we believe our strategy has satisfied the aims of the project and has provided, for a limited time period, operational guidelines that may be adopted by the relevant authorities for the reconstruction.

Acknowledgments This study was supported by DPC funds in the frame of the Task6, *Definition of Design Earthquakes for Numerical Simulations* project. We thank Dario Slejko and an anonymous reviewer for the very accurate review; their recommendations significantly improved the paper.

References

Akinci A, Malagnini L, Sabetta F (2009) Characteristics of the strong ground motions from the 6 April 2009 L'Aquila earthquake, Italy. Soil Dyn Earth Eng. doi:10.1016/j.soildyn.2009.12.006

Akkar S, Bommer JJ (2007) Prediction of elastic displacement response spectra in Europe and the Middle East. Earthq Eng Struct Dyn 36:1275–1301

Albarello D, Mucciarelli M (2002) Seismic hazard estimates from ill-defined macroseismic data at a site. Pure Appl Geophys 159(6):1289–1304

Albarello D, Bramerini F, D'Amico V, Lucantoni A, Naso G (2002) Italian intensity hazard maps: a comparison between results from different methodologies. Boll Geofis Teor Appl 43:249–262

Ambraseys NN, Free MW (1997) Surface wave magnitude calibration for European region earthquakes. J Earthq Eng 1:1–22

Ambraseys NN, Simpson KA, Bommer JJ (1996) Prediction of horizontal response spectra in Europr. Earthq Eng Struct Dyn 25(4):371–400

Anzidei M, Boschi E, Cannelli V, Devoti R, Esposito A, Galvani A, Melini D, Pietrantonio G, Riguzzi F, Sepe V, Serpelloni E (2009) Coseismic deformation of the destructive April 6, 2009 L'Aquila earthquake (central Italy) from GPS data. Geophys Res Lett 36. doi:10.1029/2009GL039145

APAT (2005) Carta Geologica d'Italia, F.o 359 L'Aquila, scale 1:50,000, APAT (Servizio Geologico d'Italia) and Regione Abruzzo, S.EL.CA, Firenze

Arias A (1970) A measure of earthquake intensity. In: Hansen R (ed) Seismic design for nuclear power plants. MIT Press, Cambridge, pp 438–483

Atzori S, Hunstad I, Chini M, Salvi S, Tolomei C, Bignami C, Stramondo S, Trasatti E, Antonioli A, Boschi E (2009) Finite fault inversion of DInSAR coseismic displacement of the 2009 L'Aquila earthquake (central Italy). Geophys Res Lett 36. doi:10.1029/2009GL039293

Azzaro R, Barbano MS, Moroni A, Mucciarelli M, Stucchi M (1999) The seismic History of Catania. J Seismol 3:235–252

Azzaro R, Barbano MS, D'Amico S, Tuvè T, Albarello D, D'Amico V (2008) Preliminary results of probabilistic seismic hazard assessment in the volcanic region of Mt. Etna (Southern Italy). Boll Geofis Teor Appl 49(1):77–91

Bazzurro P, Cornell CA (1999) Disaggregation of seismic hazard. Bull Seism Soc Am 89:501–520

Bender B, Perkins DM (1987) SEISRISK III; a computer program for seismic hazard estimation. U. S. Geological Survey, Reston 48

Bommer JJ, Douglas J, Strasser F (2003) Style-of-faulting in ground-motion prediction equations. Bull Earthq Eng 1(2):171–203

Boncio P, Lavecchia G, Pace B (2004) Defining a model of 3D seismogenic sources for Seismic Hazard Assessment applications: the case of central Apennines (Italy). J Seismol 8(3):407–425

Boncio P, Lavecchia G, Milana G, Rozzi B (2004) Seismogenesis in Central Apennines, Italy: an integrated analysis of minor earthquake sequences and structural data in the Amatrice-Campotosto area. Ann Geophys 47:1723–1742

Boncio P, Pizzi A, Brozzetti F, Pomposo G, Lavecchia G, Di Naccio D, Ferrarini F (2010) Coseismic ground deformation of the April 6th 2009 L'Aquila earthquake (central Italy, Mw6.3). Geophys Res Lett. doi:10.1029/2010GL042807

Boncio P, Tinari DP, Lavecchia G, Visini F, Milana G (2009) The instrumental seismicity of the Abruzzo Region in Central Italy (1981–2003): seismotectonic implications. Ital J Geosci (Boll Soc Geol It) 128(2):367–380

Bosi C, Galadini F, Giaccio B, Messina P, Sposato A (2003) Plio-quaternary continental deposits in the Latium-Abruzzi Apennines: the correlation of geological events across different intermontane basins. Il Quaternario 16(1Bis):55–76

Bosi C (1975) Osservazioni preliminari su faglie probabilmente attive nell'Appennino centrale. Boll Soc Geol It 94:827–859

Buccio di Ranallo (14th cent) Cronaca aquilana (1253c.-1362). In V. De Bartholomeis (ed.) Cronaca aquilana rimata di Buccio di Ranallo di Popplito di Aquila. Fonti per la storia d'Italia, Istituto Storico Italiano, Scrittori, sec. XIV, Rome, 1907, pp LXXI + 346

Castelli V, Galadini F, Galli P, Molin D, Stucchi M (2002) Caratteristiche sismogenetiche della sorgente della Laga e relazione con il terremoto del 1639.21° Convegno Nazionale GNTS Roma 19–21 novembre 2002, Roma, pp 13–16

Çelebi M, Bazzurro P, Chiaraluce L, Clemente P, Decanini L, De Sortis A, Ellsworth W, Gorini A, Kalkan E, Marcucci S, Milana G, Mollaioli F, Oliveri M, Rinaldis D, Rovelli A, Sabetta F, Stephens C (2009) Recorded motions of Mw 6.3 April 6, 2009 L'aquila Earthquake and Implications for Building Structural Damage. Earthquake Spectra (in press)

Chiarabba C, Amato A, Anselmi M, Baccheschi P, Bianchi I, Cattaneo M, Cecere G, Chiaraluce L, Ciaccio MG, De Gori P, De Luca G, Di Bona M, Di Stefano R, Faenza L, Govoni A, Improta L, Lucente FP, Marchetti A, Margheriti L, Mele F, Michelini A, Monachesi G, Moretti M, Pastori M, Piana Agostinetti N, Piccinini D, Roselli P, Seccia D, Valoroso L (2009) The 2009 L'Aquila (central Italy) MW6.3 earthquake: Main shock and aftershocks. Geophys Res Lett 36 L18308, doi:10.1029/2009GL039627

Cirella A, Piatanesi A, Cocco M, Tinti E, Scognamiglio L, Michelini A, Lomax A, Boschi E (2009) Rupture history of the 2009 L'Aquila (Italy) earthquake from non-linear joint inversion of strong motion and GPS data. Geophys Res Lett 36:L19304. doi:10.1029/2009GL039795

D'Agostino N, Avallone A, Cheloni D, D'Anastasio E, Mantenuto S, Selvaggi G (2008) Active tectonics of the Adriatic region from GPS and earthquake slip vectors. J Geophys Res 113:B12413. doi:10.1029/2008JB005860

D'Amico V, Albarello D (2003) Seismic hazard assessment from local macroseismic observation: comparison with a "standard" approach. Nat Haz 29:77–95

D'Amico V, Albarello D (2008) SASHA: a computer program to assess seismic hazard from intensity data. Seism Res Lett 79(5):663–671

D'Angeluccio F (15th cent) Cronaca delle cose dell'Aquila (1436–1485). In: Muratori LA (ed) Antiquitates Italicae Medaevi, 6, Milan, vol 174, pp 884–900

Decanini L, Gavarini C, Mollatoli F (1995) Proposta di definizione delle relazioni tra intensita' macrosismica e parametri del moto del suolo. Siena: L'ingegneria Sismica in Italia, pp 63–72

De Luca G, Marcucci S, Milana G, Sano' T (2005) Evidence of low-frequency amplification in the city of L'aquila, Central Italy, through a multidisciplinary approach including strong- and weak-motion data, ambient noise, and numerical modeling. Bull Seism Soc Am 95:1469–1481

De Tummolillis A (15th cent) Notabilia temporum. In: Corsivieri C (ed) Fonti per la storia d'Italia, Ist. Storico It, Scrittori, sec. XV, Rome, 1890, p. 96

Decreto (2008) Approvazione delle norme tecniche per le costruzioni. Gazzetta Ufficiale, n. 29 del 4.2.2008

Earthquake Research Committee (2005) Comprehensive study of probabilisitic seismic hazard map for Japan. Headquarters for Earthquake Research Promotion, Tokyo, Japan, p. 125

EMERGEO Working Group (2009) Evidence for surface rupture associated with the Mw 6.3 L'Aquila earthquake sequence of April 2009 (central Italy). Terra Nova. doi:10.1111/j.1365-3121.2009.00915.x

Falcucci E, Gori S, Peronace E, Fubelli G, Moro M, Saroli M, Giaccio B, Messina P, Naso G, Scardia G, Sposato A, Voltaggio M, Galli P. e Galadini F (2009a) The Paganica fault and surface coseismic ruptures due to the April 6, 2009 earthquake (L'Aquila, Central Italy). Seism Res Lett 80. doi:10.1785/gssrl.80.6.940

Falcucci E, Gori S, Moro M, Galadini F, Marzorati S, Ladina C, Piccarreda D, Fredi P (2009b) Evidenze di fagliazione normale tardo-olocenica nel settore compreso fra la Conca Subequana e la Media Valle dell'Aterno, a sud dell'area epicentrale del terremoto di L'Aquila del 6 Aprile 2009: implicazioni sismotettoniche. 28° convegno nazionale GNGTS, Trieste, 16–19 November 2009, pp 161–163

Field EH, Dawson TE, Felzer KR, Frankel AD, Gupta V, Jordan TH, Parsone T, Petersen MD, Stein RS, Weldon RJ, Wills CJ (2009) Uniform California earthquake rupture forecast, version 2 (UCERF 2). Bull Seismol Soc Am 99(4):2053–2107

Galadini F, Galli P (1999) The Holocene paleoearthquakes on the 1915 Avezzano earthquake faults (central Italy); implications for active tectonics in the central Apennines. Tectonophysics 308:143–170

Galadini F, Galli P (2000) Active tectonics in the Central Apennines (Italy)—input data for Seismic Hazard Assessment. Nat Haz 22:225–270

Galadini F, Galli P (2003) Paleoseismology of silent faults in the Central Apennines (Italy): the Mt. Vettore and Laga Mts. faults. Ann Geophys 5:815–836

Galadini F, Galli P, Moro M (2003) Paleoseismology of silent faults in the central Apennines (Italy): the Campo Imperatore fault (Gran Sasso Range fault system). Ann Geophys 46:793–813

Galli P, Galadini F, Moro M, Giraudi C (2002) New paleoseismological data from the Gran Sasso d'Italia area (central Apennines) Geoph Res Lett 29 (7). doi:10.1029/2001GL013292

Galli P, Naso G (2009) Unmasking the 1349 earthquake source (southern Italy). Paleoseismological and archaeoseismological indications from the Aquae Iuliae fault. J Struct Geol 31:128–149

Galli P, Camassi R, Azzaro R, Bernardini F, Castenetto S, Molin D, Peronace E, Rossi A, Vecchi M, Tertulliani A (2009) Il terremoto aquilano del 6 aprile 2009: rilievo macrosismico, effetti di superficie ed implicazioni sismotettoniche. Il Quaternario 22(2):235–246

Galli P, Galadini F, Pantosti D (2008) Twenty years of paleoseismology in Italy. Eart Sci Rev. doi:10.1016/j.earseirev.2008.01.001

Galli P, Giaccio B, Messina P (2010) The 2009 central Italy earthquake seen through 0.5 myr-long tectonic history of the L'aquila faults system. J Quaternary Sci Rev. doi:10.1016/j.quascirev.2010.08.018

Giraudi C, Frezzotti M (1995) Palaeoseismicity in the Gran Sasso Massif (Abruzzo, central Italy). Quatern Int 25:81–93

Gomez Capera AA, D'Amico V, Meletti C, Rovida A, Albarello D (2010) Seismic hazard assessment in terms of macroseismic intensity in Italy: a critical analysis from the comparison of different computational procedures. Bull Seism Soc Am (in press)

Gori S, Giaccio, Galadini F, Falcucci E, Messina P, Sposato A, Dramis F (2009) Active normal faulting along the Mt. Morrone south-western slopes (central Apennines, Italy). Int J Earth Sci (Geol Rundsch). doi:10.1007/s00531-009-0505-6

Gori S, Galadini F, Galli P, Giaccio B, Messina P, Sposato A, Falcucci E, Dramis F (2010) Active normal faulting and large scale gravitational deformation: the case of the Mt. Morrone SW slopes (central Apennines, Italy). Rend Online Soc Geol It 11:23

Gorini A, Nicoletti M, Marsan P, Bianconi R, De Nardis R, Filippi L, Marcucci S, Palma F, Zambonelli E (2010) The Italian strong motion network. Bull Earthq Eng. doi:10.1007/s10518-009-9141-6

Grant DN, Bommer JJ, Pinho R, Calvi GM, Goretti A, Meroni F (2007) A Prioritization Scheme for Seismic Intervention in School Buildings in Italy. Earthquake Spectra 23. doi:10.1193/1.2722784

Gruppo di lavoro MS (2008) Indirizzi e criteri per la microzonazione sismica. Conferenza delle Regioni e delle Province autonome—Dipartimento della protezione civile, Roma, 3 vol. e Dvd

Harmsen S, Frankel A (2001) Geographic deaggregation of seismic hazard in the United States. Bull Seism Soc Am 91:13–26

Housner GW (1952) Spectrum intensities of strong motion earthquakes. Proceedings of Symposium on Earthquake and Blast Effects on Structures. Earthquake Engineering Research Institute

LaForge R (1996) Implementation of SEISRISK III, USGS, Colorado, Boulder, Open File

Lavecchia G, Brozzetti F, Barchi M, Keller J, Menichetti M (1994) Seismotectonic zoning in East-Central Italy deduced from the analysis of the Neogene to present deformations and related stress fields. Soc Geol Am Bull 106:1107–1120

Magri L, Mucciarelli M, Albarello D (1994) Estimates of site seismicity rates using ill-defined macroseismic data. PAGEOPH 143:618–632

Margottini C, Molin D, Serva L (1992) Intensity versus ground motion: a new approach using Italian data. Eng Geol 33:45–58

Matthews MV, Ellsworth WL, Reasenberg PA (2002) A Brownian model for recurrent earthquakes. Bull Seism Soc Am 92:2233–2250

McGuire RK (1995) Probabilistic seismic hazard analysis and design earthquakes: closing the loop. Bull Seism Soc Am 85:1275–1284

Messina P, Galli P, Falcucci E, Galadini F, Giaccio B, Gori S, Peronace E, Sposato A (2009) Evoluzione geologica e tettonica quaternaria dell'area interessata dal terremoto aquilano del 2009. Geoitalia 28:24–29

Messina P, Galli P, Giaccio B, Peronace E (2009b) Quaternary tectonic evolution of the area affected by the Paganica fault (2009 L'Aquila earthquake). 28° convegno nazionale GNGTS, Trieste, 16–19 November 2009, pp 47–50

Michetti AM, Brunamonte F, Serva L, Vittori E (1996) Trench investigations of the 1915 Fucino earthquake fault scarps (Abruzzo, central Italy): geological evidence of large historical events. J Geophys Res 101:5921–5936

Moro M, Bosi V, Galadini F, Galli P, Giaccio B, Messina P, Sposato A (2002) Analisi paleosismologiche lungo la faglia del M. Marine (alta valle dell'Aterno): risultati preliminari. Il Quaternario 15:267–278

Mucciarelli M, Albarello D, D'Amico V (2008) Comparison of Probabilistic Seismic Hazard estimates in Italy. Bull Seism Soc Am 98(6): 2652–2664. doi:10.1785/0120080077

Mucciarelli M, Peruzza L, Caroli P (2000) Tuning of seismic hazard estimates by means of observed site intensities. J Earth Eng 4:141–159

Musson RMW (2009) Ground motion and probabilistic hazard. Bull Earthq Eng 7:575–589

Pace B, Boncio P, Brozzetti F, Lavecchia G, Visini F (2008) From regional seismic hazard to scenario earthquake for seismic microzoning. A new methodological approach for the Celano project. Soil Dyn Earthq Eng 28:866–874

Pace B, Boncio P, Lavecchia G (2002) The 1984 Abruzzo earthquake (Italy): an example of seismogenic process controlled by interaction between differently-oriented sinkinematic faults. Tectonophysics 350:237–254

Pace B, Peruzza L, Lavecchia G, Boncio P (2006) Layered Seismogenic Source Model and Probabilistic Seismic-Hazard Analyses in Central Italy. Bull Seism Soc Am 96(1):107–132

Pace B, Peruzza L, Visini F (2010) LASSCI2009.2: Layered Earthquake Rupture Forecast model for central Italy submitted to CSEP project Annals of Geophysics 53(3):85–97

Pantosti D, D'Addezio G, Cinti FR (1996) Paleoseismicity of the Ovindoli-Pezza fault, central Apennines, Italy: A history including a large, previously unrecorded earthquake in the Middle ages (860-1300 A.D.). J Geophys Res 101:5937–5959

Pasquale V, Verdoya M, Chiozzi P, Ranalli G (1997) Rheology and seismotectonic regime in the northern central Mediterranean. Tectonophysics 270:239–257

Petersen MD, Frankel AD, Harmsen SC, Mueller CS, Haller KM, Wheeler RL, Wesson RL, Zeng Y, Boyd OS, Perkins DM, Luco N, Field EH, Wills CJ, Rukstales KS (2008) Documentation for the 2008 Update of the United States National Seismic Hazard Maps. U.S. Geological Survey, Open-File Report 2008–1128, 61 p

Peruzza L, Pace B, Cavallini F (2010) Error propagation in time-dependent probability of occurrence for characteristic earthquakes in Italy. J Seismol. doi:10.1007/s10950-008-9131-1

Peruzza L, Pace B (2002) Sensitivity analysis for seismic source characteristics to probabilistic seismic hazard assessment in central Apennines (Abruzzo area). Boll Geofis Teor Appl 43:79–100

Peruzza L, Pace B, Lavecchia G, Boncio P (2007) Reply to "Comment on 'Layered Seismogenic Source Model and Probabilistic Seismic-Hazard Analyses in Central Italy' by Pace B, Peruzza L, Lavecchia G, Boncio P " by Marzocchi, W. Bull Seism Soc Am 97(5):1766–1768

Peruzza L, Pace B, Visini F (2011) Fault-based earthquake rupture forecast in Central Italy: remarks after the L'Aquila Mw 6.3 event. Bull Seism Soc Am 101(1) (in press)

Piccardi L, Gaudemer Y, Tapponier P, Boccaletti M (1999) Active oblique extension in the central Apennines (Italy); evidence from the Fucino region. Geophys J Int 139(2):499–530

Pondrelli S, Salimbeni S, Morelli A, Ekstrom G, Olivieri M, Boschi E (2009) Seismic moment tensors of the April 2009, L'Aquila (Central Italy), earthquake sequence. Geophys J Int. doi:10.1111/j.1365-246X.2009.04418.x

Pondrelli S, Salinbeni S, Ekström G, Morelli A, Gasperini P, Vannucci G (2006) The Italian CMT dataset from 1977 to present. Phys Earth Planet Inter 159:286–303

Rossi A, Tertulliani A, Vecchi M (2005) Studio macrosismico del terremoto aquilano del 24 giugno 1958. Il Quaternario 18(2):101–112

Sabetta F, Lucantoni A, Bommer J, Bungum H (2005) Sensitivity of PSHA results to ground motion prediction relations and logic-tree weights. Soil Dyn Earthq Eng 25(4):317–329

Sabetta F, Pugliese A (1996) Estimation of response spectra and simulation of non-stationary earthquake ground motions. Bull Seism Soc Am 86(2):337–352

Salvi S, Cinti FR, Colini L, D'Addezio G, Doumaz F, Pettinelli E (2003) Investigation of the active Celano-L'Aquila fault system, Abruzzi (central Apennines, Italy) with combined ground-penetrating radar and paleoseismic trenching. Geophys J Int 155:805–818

Scherbaum F, Schmedes J, Cotton F (2004) On the conversion of source-to-site distance measures for extended earthquake source models. Bull Seism Soc Am 94(3):1053–1069

Schnabel B, Lysmer J, Seed HB (1972) SHAKE—A computer program for earthquake response analysis of horizontally layered sites. EERC Report No 72-12

Schorlemmer D, Jordan TH, Zechar JD, Maechling PJ, Gerstenberger M, Wiemer S (2006) Collaboratory for the Study of Earthquake Predictability (CSEP). American Geophysical Union, Fall Meeting 2006, abstract #S12A-01, http://www.cseptesting.org/documents/talks

Schorlemmer D, Jackson DD, Zechar JD, Jordan TH (2009) Collaboratory for the Study of Earthquake Predictability: Design of Prediction Experiments. American Geophysical Union, Fall Meeting 2009, abstract #NH13A-1133

Selvaggi G (1998) Spatial distribution of horizontal seismic strain in the Apennines from historical earthquakes. Ann Geofisis 41:241–251

Stucchi M, Camassi R, Rovida A, Locati M, Ercolani E, Meletti C, Migliavacca P, Bernardini F, Azzaro R (2007) DBMI04, il database delle osservazioni macrosismiche dei terremoti italiani utilizzate per la compilazione del catalogo parametrico CPTI04. http://emidius.mi.ingv.it/DBMI04/

Tertulliani A, Rossi A, Cucci L, Vecchi M (2009) L'Aquila (Central Italy) Earthquake: the Predecessors of the April 6, 2009 Event. Historical Seismologist. doi:10.1785/gssrl.80.6.1008

Trifunac MD, Brady AG (1975) A study of the duration of strong earthquake ground motion. Bull Seism Soc Am 65:581–626

Vanmarcke EH, Lai SP (1980) Strong-motion duration and RMS amplitude of earthquake records. Bull Seism Soc Am 70(4):1293–1307

Vezzani L, Ghisetti F (1998) Carta Geologica dell'Abruzzo, 1:100,000 scale. S.EL.CA, Firenze

Walters RJ, Elliott JR, D'Agostino N, England PC, Hunstad I, Jackson JA, Parsons B, Phillips RJ, Roberts G (2009) The 2009 L'Aquila earthquake (central Italy): a source mechanism and implications for seismic hazard. Geophys Res Lett 36:L17312. doi:10.1029/2009GL039337

Wells DL, Coppersmith KJ (1994) New empirical relationships among magnitude, rupture length, rupture width, rupture area, and surface displacement. Bull Seism Soc Am 84:974–1002

Working Group CPTI (2004) Catalogo Parametrico dei Terremoti Italiani, versione 2004 (CPTI04), INGV-Bologna, available on-line at: http://emidius.mi.ingv.it/CPTI

Working Group MPS (2004) Redazione della mappa di pericolosità sismica prevista dall'Ordinanza PCM 3274 del 30 marzo 2003, Rapporto conclusivo per il Dipartimento di Protezione Civile, INGV, Editor, Milano-Roma